

# An integrative taxonomic framework for the study of the genus *Ciona* (Ascidiacea) and description of a new species, *Ciona intermedia*

FRANCESCO MASTROTOTARO<sup>1,2</sup>, FEDERICA MONTESANTO<sup>1,2,\*</sup>, MARIKA SALONNA<sup>3</sup>, FRÉDÉRIQUE VIARD<sup>4</sup>, GIOVANNI CHIMIENTI<sup>1,2</sup>, EGIDIO TRAINITO<sup>5</sup> and CARMELA GISSI<sup>2,3,6,\*</sup>

<sup>1</sup>Dipartimento di Biologia, Università degli Studi di Bari 'Aldo Moro', Via Orabona, 4, 70125 Bari, Italy

<sup>2</sup>CoNISMa, Consorzio Nazionale Interuniversitario per le Scienze del Mare, Piazzale Flaminio 9, 00197, Roma, Italy

<sup>3</sup>Dipartimento di Bioscienze, Biotecnologie and Biofarmaceutica, Università degli Studi di Bari 'Aldo Moro', Via Orabona, 4, 70125 Bari, Italy

<sup>4</sup>Sorbonne Université, CNRS, Laboratory of Adaptation & Diversity in Marine Environment (UMR 7144), Station Biologique, Roscoff, France

<sup>5</sup>Villaggio I Fari, Loiri Porto San Paolo, Olbia-Tempio, Italy

<sup>6</sup>IBIOM, Istituto di Biomembrane, Bioenergetica e Biotecnologie Molecolari, CNR, Bari, Via Amendola 165/A, 70126 Bari, Italy

Received 7 June 2019; revised 12 February 2020; accepted for publication 30 March 2020

The genus *Ciona* is an interesting 'taxonomic case' because its evolutionary history and taxonomy have not yet been resolved completely. In this study, we present new findings, describing specimens of an unidentified *Ciona* species collected along the north-eastern coasts of Sardinia (Tyrrhenian Sea, Mediterranean Sea). Applying an integrative taxonomic approach, based on the joint examination of morphological and molecular traits, we identify these specimens as a new species, *Ciona intermedia* sp. nov. Morphological comparisons and peculiarities of the habitat first revealed that these *Ciona* specimens have intermediate characters compared with other *Ciona* species. Molecular characterization (based on three mitochondrial regions: two already used for discriminating *Ciona* cryptic species and a newly developed one) confirmed that our specimens could not be assigned to any previously molecularly-characterized species. Both molecular phylogenetic reconstructions and morphological data clearly indicate *C. intermedia* as sister clade of *Ciona edwardsi*. Our findings add further complexity to the taxonomy of *Ciona*, underlying the importance of an integrative taxonomic approach for the study of the evolutionary history of this enigmatic genus.

ADDITIONAL KEYWORDS: DNA barcode – Mediterranean Sea – mitochondrial genes – model organism.

## INTRODUCTION

The genus *Ciona* Fleming, 1822 includes several species used as model organisms in various research fields, from evolutionary developmental biology to chordate evolution

(Millar, 1953; Dehal *et al.*, 2002; Cañestro *et al.*, 2003; Satoh *et al.*, 2003). Its suitability as model organism is attributable to anatomical and molecular features of this genus, such as the relatively large size, the transparency of the tunic, the macroscopic internal anatomy, the easily detected reactions to external stimuli (Millar, 1953), the small, compact genome and the availability of powerful experimental tools for molecular studies (Lemaire, 2011). More recently, this genus has also become a case study for ecological studies (Procaccini *et al.*, 2011; Zhan *et al.*, 2015), notably because two species, namely *Ciona intestinalis* (Linnaeus, 1767) and *Ciona robusta* Hoshino & Tokioka,

\*Corresponding authors. E-mail: federica.montesanto@uniba.it; carmela.gissi@uniba.it

[Version of record, published online 29 May 2020; <http://zoobank.org/urn:lsid:zoobank.org:pub:C7FA4AD8-82FA-4BCE-A12B-FF3F648F1FB8>]

1967 (formerly known as *C. intestinalis* type B and *C. intestinalis* type A, respectively), have been recognized as invasive species in several regions worldwide (see [Bouchemousse et al., 2016a](#): supplementary material). Nevertheless, this genus represents a ‘taxonomic case’ because its assignment at order level is still debated, there are strong difficulties in delineation and delimitation of the various species, and the genus has a complex evolutionary history. The genus *Ciona* is currently placed in the order Phlebobranchia based on the presence of a large pharynx with inner longitudinal vessels ([Monniot, 1991](#)). In the past, it was included in the order Aplousobranchia ([Kott, 1990, 2005](#)) on the basis of its vanadium oxidation state ([Hawkins et al., 1983](#)) and based on the regenerative role of its epicardial tissue ([Kott, 1990](#)). More recently, some molecular phylogenetic reconstructions supported a sister relationship of the genus *Ciona* with Aplousobranchia ([Turon & López-Legentil, 2004](#); [Shenkar et al., 2016](#)), although sometimes with an unstable positioning (see discussion by [Shenkar et al., 2016](#)).

As for the difficulties in species delineation, since the study by [Berrill \(1950\)](#), several *Ciona* species were synonymized with the type species *C. intestinalis*, until, in the early 2000s, molecular studies indicated the existence of a surprisingly high genetic divergence among specimens of *C. intestinalis* from distant geographical localities ([Suzuki et al., 2005](#); [Caputi et al., 2007](#); [Iannelli et al., 2007](#); [Nydham & Harrison, 2007, 2010](#); [Zhan et al., 2010](#); [Sato et al., 2012](#)). These findings led first to the description of *C. intestinalis sensu lato* as a complex of four cryptic species, named from A to D, and then to in-depth morphological analyses revealing that *C. intestinalis* type A is *C. robusta*, whereas *C. intestinalis* type B corresponds to *C. intestinalis sensu stricto* ([Brunetti et al., 2015](#); [Pennati et al., 2015](#)). In addition, no introgression has been reported between the two species in sympatric areas, proving the existence of reproductive barriers between the two taxa ([Bouchemousse et al., 2016b, c](#); [Malfant et al., 2018](#)). The current knowledge therefore indicates that *C. robusta* and *C. intestinalis* are clearly distinguishable by the morphology of both adults and larvae as well as by their genetic background and geographical distribution. On the contrary, *Ciona* sp. C and *Ciona* sp. D still lack morphological diagnostic characters and can be identified currently only through molecular analyses ([Nydham & Harrison, 2007, 2010](#); [Zhan et al., 2010](#); [Brunetti et al., 2015](#)).

Another peculiar case is represented by *Ciona roulei* Lahille, 1890, for which we need to clarify that the original binomial of this species was *Ciona roulii* Lahille, 1890, and that [Brunetti et al., \(2015\)](#) considered the binomial *C. roulei* as an ‘incorrect subsequent spelling’ ([ICZN, 1999](#): article 33.3) introduced by Hartmeyer (1909–1911) and [Harant & Vernières](#)

(1933) without a clear justification. Nonetheless, the *C. roulii* binomial was clearly created by Lahille in homage to Roule (author of many ascidian species from 1883 to 1887), thus it can be considered an inadvertent misspelling ([ICZN, 1999](#): article 32.5). Moreover, the *C. roulei* binomial has been in prevailing usage by all subsequent authors ([ICZN, 1999](#): article 33.3.1; i.e. [Harant & Vernières, 1933](#)). Therefore, here we have chosen to maintain the spelling *C. roulei*.

Mitochondrial phylogenetic analyses did not distinguish between *C. roulei* and *C. intestinalis*, and the two taxa hybridize with a high rate of success in both directions, displaying survival and growth rates similar to those found in respective intraspecific crosses ([Malfant et al., 2018](#)). Therefore, further in-depth investigations, integrating different types of data and different methodologies, are needed to confirm or exclude the taxonomic validity of *C. roulei*. It should also be noticed that the usage of the biological species concept should be examined carefully in the genus *Ciona*. For instance, *in vitro* crosses and first-generation hybrids can be produced among accepted species, such as *C. intestinalis* and *C. robusta* ([Sato et al., 2014](#); [Bouchemousse et al., 2016b](#); [Malfant et al., 2018](#)), two taxa that introgressed in the past ([Roux et al., 2013](#)). Studies of natural populations have shown that hybridization is not followed by successful introgression ([Bouchemousse et al., 2016c](#)), suggesting the existence of reproductive barriers between the two species in the wild. On the contrary, *Ciona edwardsi* Roule, 1884 has complete reproductive isolation from *C. intestinalis*, *C. robusta* and *C. roulei* ([Lambert et al., 1990](#); [Malfant et al., 2018](#)). These case studies show the complexity of the evolutionary history and speciation processes in this genus that can obscure complicated taxonomic and systematics studies. Altogether, these results point to the *Ciona* genus as a complex taxonomic group that needs to be studied according to an integrative taxonomic approach ([Padial et al., 2010](#)). In fact, the intricate evolutionary history and the possible presence of ongoing speciation events require the combination of different types of data and the usage of different methodologies for species delineation.

In this study, we report the identification of several specimens of *Ciona* with previously undescribed features found along the north-eastern coasts of Sardinia. The integrative taxonomic approach taken below reveals that these specimens belong to a new species that is described in detail by morphological, ecological and molecular traits. Furthermore, molecular phylogenetic reconstructions of the genus *Ciona* based on three mitochondrial regions have allowed identification of the species *C. edwardsi* as the closest relative of this new species. These data provide an important contribution to the knowledge of the evolutionary history of *Ciona*.

## MATERIAL AND METHODS

## SAMPLING AND MORPHOLOGICAL ANALYSIS

Seven specimens of *Ciona* sp. were photographed and collected manually by SCUBA diving near Olbia (Sardinia, Tyrrhenian Sea, Italy) at a depth of 3–5 m in July 2014. The sampling area was mainly characterized by calcareous algae, large solitary ascidians belonging to the genera *Phallusia* and *Pyura* and small colonial ascidians, such as *Symplegma brakenhielmi* (Michaelsen, 1904) (Mastrototaro *et al.*, 2019). Specimens of *Ciona* sp. were collected from shady sites, such as crevices of the rocks and under the pebbles. Five specimens were preserved directly in 99% ethanol for molecular investigation. The other specimens were narcotized with menthol crystals in seawater and then preserved in a 5% formaldehyde solution in seawater for morphological analyses. In the relaxed specimens, the tunic was removed, and the body was coloured with Mayer's Haemalum solution for detailed investigations. We considered numerous morphological characters (i.e., consistency of tunic, morphology of siphons, number and distribution of body muscles, structure of pharynx, shape of stomach and gonads) and also some ecological characteristics of the specimens (i.e., occurrence in light or shady sites).

*Ciona* specimens from Olbia were compared morphologically with specimens of *C. edwardsi*, *C. intestinalis* and *C. robusta* in the private collection of the Laboratory of Zoology of F. Mastrototaro (available on request; see Supporting Information, Table S1).

## MOLECULAR ANALYSES

Total DNA of the three *Ciona* sp. specimens preserved in ethanol (labels 'CR', 'Ca' and 'Cb' in the Supporting Information, Tables S2–S4) was extracted from muscle tissue using a modified cetyl trimethylammonium bromide (CTAB) method (Hirose & Hirose, 2009). DNA from two *C. roulei* and three *C. edwardsi* specimens, sampled at Banyuls-sur-Mer (France), were also analysed. These *C. roulei* and *C. edwardsi* DNAs were obtained as part of an earlier study on experimental crosses in the genus *Ciona* (Malfant *et al.* 2018), during which the specimen identification was made by those authors based on morphological criteria, i.e. the external morphology, the spermiduct and gonoduct features and the larvae (see data in the supplementary material of Malfant *et al.*, 2018). The experimental crosses and the molecular analyses performed on those *C. roulei* and *C. edwardsi* specimens by Malfant *et al.*, (2018) and in an ongoing genetic (nuclear-based) study (M. Malfant, E. Pante, C. Daguin-Thiébaud, C. Roby & F. Viard, unpublished observations.) matched the expectations based on the morphological identifications.

Using the primer pairs reported in Table 1, three mitochondrial (mt) regions were amplified: (1) a fragment of the *cox1* gene ~1.2 kb long, named COI-1.2kb, containing the 650-bp-long region widely used as a reliable DNA barcode; (2) a fragment comprising the *cox2* (cytochrome oxidase subunit 2) and *cob* (cytochrome *b*) genes, named x2cb; and (3) a fragment, named x3n1, encompassing the three genes *cox3* (cytochrome oxidase subunit 3), *trnK* (tRNA-Lys) and *nad1* (NADH dehydrogenase subunit 1), and two non-coding spacers. This fragment was originally identified and used by Iannelli *et al.*, (2007) as a mt region able to distinguish *C. intestinalis* (formerly known as *C. intestinalis* type B) from *C. robusta* (formerly known as *C. intestinalis* type A), and then it was demonstrated also to be able to distinguish sp. C and sp. D (Zhan *et al.*, 2010). The COI-1.2kb fragment was amplified in all specimens (three *Ciona* sp., two *C. roulei* and three *C. edwardsi*), whereas x3n1 was amplified in the three *Ciona* sp. specimens and in only one representative of *C. roulei* and *C. edwardsi* each. The three analysed *Ciona* sp. had identical COI-1.2kb and x3n1 sequences. Finally, x2cb was amplified in one specimen for each of the three species considered (*Ciona* sp., *C. roulei* and *C. edwardsi*).

The COI-1.2kb fragment was amplified with the high-fidelity PrimeStar HS DNA polymerase (Takara Bio Inc.) in a 25 µL reaction volume containing: 1× reaction buffer with 1 mM final concentration of MgCl<sub>2</sub> (Takara Bio Inc.), 0.2 mM of each dNTP, 0.3 µM of each primer and 1.25 units of PrimeStar HS DNA polymerase (Takara Bio Inc.). Amplification conditions were as follows: 30 cycles with denaturation for 10 s at 98 °C, annealing for 15 s at 46–52 °C (depending on the specimen), extension for 2 min at 72 °C and a final elongation step of 5 min at 72 °C.

Amplifications of the x2cb fragment were performed according to a long-range polymerase chain reaction protocol, because the frequent rearrangements of the gene order typical of the ascidian mt genome (Gissi *et al.*, 2010) make it impossible to predict a priori the distance between the *cox2* and *cob* genes in the studied *Ciona* taxa. Therefore, amplification of the x2cb fragment was carried out with the high-fidelity LA Taq DNA polymerase (Takara Bio Inc.) in the following conditions: an initial denaturation for 1 min at 94 °C, then 30 amplification cycles (denaturation for 10 s at 98 °C, annealing for 5 s at 50 °C and extension for 12 min at 68 °C) and a final elongation step of 10 min at 72 °C. The reactions were carried out in a final volume of 25 µL containing: 1× reaction buffer with 2.5 mM final concentration of MgCl<sub>2</sub> (Takara Bio Inc.), 0.4 mM of each dNTP, 0.2 µM of each of the two primers and 1.25 units of LA Taq DNA polymerase (Takara Bio Inc.).

**Table 1.** Mitochondrial regions and primers used in this study

Fragment name	Primer pair	Length (kb)*	Primer name	Sequence (5' → 3')	Notes/reference
COI-1.2kb	dinF/ConsR1	1.2	dinF consR1 <sup>†</sup>	CGTTGRTTTATRTCTACwAATCATAARGA CATTGATYYCCTCTTTTACTAGATTAAGTTTT	Brunetti <i>et al.</i> (2017) Present study
x2cb	ux2F/ucbR	1.1	ux2F ucbR	GYAGTTRGDCAVCARTGATATTG GGAATASAYCGTAAAATVGCATARGC	Iannelli <i>et al.</i> (2007) Iannelli <i>et al.</i> (2007)
x3n1	tx3F/tn1R	0.6–0.7	tx3F tn1R	GAGTGTGCKATTTGTGTTATGAC ATYTGAGCYACTCCTCGAATTC	Iannelli <i>et al.</i> (2007) Iannelli <i>et al.</i> (2007)

\*Average range for the known *Ciona* species.

<sup>†</sup>consR1 is a modification of the 'consensus R' primer of Nydam & Harrison (2007), obtained by deleting three nucleotides at the 5' end and the last nucleotide at the 3' end, corresponding to a third codon position of *cox1*.

The x3n1 fragment was amplified with the DreamTaq polymerase (Thermo Fisher Scientific) in a final volume of 25 µL containing: 1× reaction buffer with 2 mM final concentration of MgCl<sub>2</sub> (Thermo Scientific), 0.2 mM of each dNTP, 0.5 µM of each of the two primers and 1.25 units of DreamTaq polymerase. The amplification conditions were as follows: an initial denaturation for 3 min at 95 °C, then 30 amplification cycles (denaturation for 30 s at 95 °C, annealing for 30 s at 50 °C, extension for 2 min at 72 °C) followed by a final elongation step of 5 min at 72 °C.

All amplicons obtained were purified with the DNA Clean&Concentrator kit (Zymo Research) and sequenced directly according to the Sanger method at the Microsynth AG (Switzerland) or Eurofins Genomics (Germany). Quality checking and sequence assembly were carried out with Geneious v.5.5.7.2 (<http://www.geneious.com>; Kearse *et al.*, 2012). All sequences were deposited in the European Nucleotide Archive (ENA) database and their accession numbers are reported in the Supporting Information (Tables S2–S4).

For comparative analyses, homologous sequences of the genus *Ciona* were searched in the National Center for Biotechnology Information non-redundant nucleotide database (nr-nt db, on 1 February 2019) by BLASTN (Altschul *et al.*, 1990), using our *Ciona* sp. sequences as the query. Concerning *cox1*, we analysed a final dataset consisting of the following: representative sequences of *C. robusta* and *C. intestinalis* included in the study by Malfant *et al.* (2018); three sequences of *Ciona* sp. C and *C. sp. D* from another unpublished study (M. Malfant, E. Pante, C. Daguin-Thiébaud, C. Roby, F. Viard, unpublished observations); and all other *Ciona* species whose sequences were available in nr-nt db. The analysed sequences of *cox1*, x2cb and x3n1 are listed in the Supporting Information (Tables S2, S3 and S4, respectively).

Phylogenetic analyses were performed separately for the three mt regions. Sequences were aligned by hand or with MAFFT (Katoh *et al.*, 2002), preserving the codon structure of the protein-coding genes. The final alignment of *cox1* was 1575 bp long (with 737 sites without gaps in 87% of the sequences) and consisted of 54 *Ciona* sequences plus a sequence of *Clavelina lepadiformis* (Müller, 1776) used as the outgroup (see Supporting Information, Table S2). The final alignment of x2cb was 1127 bp long (with 1078 ungapped sites) and consisted of nine *Ciona* sequences plus five Aplousobranchia species as outgroups (see Supporting Information, Table S3). The final alignment for x3n1 was 676 bp long (with 502 ungapped sites) and consisted of 19 *Ciona* sequences (see Supporting Information, Table S4). *Ciona savignyi* Herdman, 1882 *sensu* Roule, 1884 was not included in the x3n1 alignment because in this species the *nad1* gene is not adjacent to *cox3-tnK*.

Phylogenetic reconstructions were performed with the maximum likelihood (ML) method and by Bayesian inference (BI). For ML, we used the online PhyML-SMS v.3.0 software, which includes the automatic model selection by Smart Model Selection (SMS) (Guindon & Gascuel, 2003; Lefort *et al.*, 2017; <http://www.atgc-montpellier.fr/phyml-sms/>). The best-fitting substitution model selected under the Akaike information criterion (AIC) was GTR+I+G for both the *cox1* and the x2cb alignments, and TN93+G for the x3n1 alignment. The proportion of invariant sites (I) and the gamma shape parameter (alpha) for the four rate categories were estimated by the PhyML v.3.0 software. Bootstrap values, indicating node reliability, were based on 100 replicates. Bayesian trees were inferred with MrBayes v.3.2.7a (Ronquist *et al.*, 2012). The BI analyses were performed using the model already selected by PhyML-SMS. However, the more general GTR+G model was used for the x3n1 alignment instead of TN93+G, because this last model is not implemented in MrBayes. Two parallel analyses, each composed of one cold and three incrementally heated chains, were run for 1 000 000 generations. Trees were sampled every 100 generations, and the results of the initial 250 000 generations were discarded (burn-in fraction of 25%), after verifying that stationarity of the logarithm of Likelihood was reached. The potential scale reduction factor (PSRF) was also checked as convergent diagnostic, according to the indications reported in the MrBayes manual. Therefore, a total of 7500 trees were used to calculate the Bayesian posterior probabilities (BPPs) at the different nodes.

Species delimitation analyses were carried out with two methods based on completely different approaches: the automatic barcode gap discovery (ABGD) method (Puillandre *et al.*, 2012), a sequence similarity clustering method; and the Poisson tree processes (PTP; Zhang *et al.*, 2013), a tree-based coalescence method. ABGD clusters sequences into partitions, consisting of hypothetical species, based on the statistical inference of the 'barcode gap', i.e. the gap in the distribution of intraspecies and interspecies pairwise distances. On the contrary, PTP infers putative species boundaries on a non-ultrametric input tree assuming the existence of two independent classes of Poisson processes, one describing speciation and the other coalescent events. The hypothetical species identified by the two methods are hereafter referred to as operational taxonomic units (OTUs). These methods were applied only to the *cox1* and x3n1 datasets, because they consist of at least three sequences for most species, a number suitable for the species delimitation analyses.

The ABGD analyses were performed on the Web-based interface <http://www.wabi.snv.jussieu.fr/public/abgd/> (Puillandre *et al.*, 2012), initially using the default

values for both the proxy of the minimum relative gap width ( $X = 1.5$ ) and the scanned range of prior intraspecific divergence ( $P_{\min}$ – $P_{\max} = 0.001$ – $0.1$ , with  $P$  = prior intraspecific divergence). Then, the robustness of the ABGD results was checked by changing the parameter values one at a time, in particular by increasing  $P_{\max}$  (to 0.2 or 0.3) in order to account for the fast substitution rate typical of ascidians (Yokobori *et al.*, 1999; Tsagkogeorga *et al.*, 2010; Rubinstein *et al.*, 2013) and by decreasing/increasing  $X$  (to 1, 2, 3) in order to verify the existence/avoid smaller local gaps. For each value of  $X$  and  $P_{\max}$ , the pairwise distances were calculated according to the three nucleotide substitution models available in ABGD: Jukes–Cantor (JC; Jukes & Cantor, 1969), Kimura two-parameter (K2P; Kimura, 1980) and uncorrected p-distances (p-dist). This strategy allowed the exclusion of possible bias of the selected evolutionary model on the OTU delimitation. Therefore, a total of 18 ABGD analyses were performed per alignment.

Given that our *cox1* alignment contains several missing data, i.e. gapped sites related to the different lengths of the sequences available in nr-nt db (see Supporting Information, Table S2), to exclude potential bias attributable to these sites, the ABGD analyses were carried out on the following four *cox1* alignments (without outgroup), consisting of: (1) all the 1566 (gapped plus ungapped) sites of all 54 *Ciona* sequences (1566-All); (2) only the 451 ungapped sites present in all 54 *Ciona* sequences (451-Nogap-All); (3) 737 ungapped sites obtained after excluding the seven shortest *Ciona* sequences (737-Nogap-47taxa; for the excluded taxa, see Supporting Information, Table S2); and (4) 1084 sites, with only six gapped sites, obtained by considering only the 12 longest *Ciona* sequences (1084-12taxa). Thus, this alignment includes only one or two sequences per species (for the included taxa, see Supporting Information, Table S2). The x3n1 alignment was analysed as it is, including gapped sites, because in this case the gapped sites correspond to real insertions/deletions, not to missing data.

The PTP method (Zhang *et al.*, 2013) was applied to the *cox1* and x3n1 datasets using as input both the ML and the Bayesian tree, although PTP was demonstrated to be robust to different tree reconstruction methods (Tang *et al.*, 2014). The Bayesian implementation of the PTP (bPTP) was performed through the Web interface <http://species.h-its.org/ptp/> (Zhang *et al.*, 2013), removing the outgroup and using the following parameters: 500 000 Markov chain Monte Carlo (MCMC) generations, thinning every 100 generations and a burn-in fraction of 0.20. The convergence of the MCMC chains was confirmed by visual inspection of the likelihood plot, as reported in the PTP help (<https://species.h-its.org/help/>), and the maximum likelihood solution was recorded.

## RESULTS

Based on our integrative taxonomic approach, we can hypothesize confidently that the collected specimens belong to a new species that we describe below. In our approach, we consider numerous morphological characters, some ecological characteristics and three molecular markers: two mitochondrial regions (COI-1.2kb and x3n1) already used successfully for discriminating cryptic species within the so-called *Ciona intestinalis* species complex (Iannelli *et al.*, 2007; Nydam & Harrison, 2007; Zhan *et al.*, 2010) and the new fragment x2cb, examined here for the first time for reconstructing the phylogeny of the genus *Ciona*.

## TAXONOMY

FAMILY CIONIDAE LAHILLE, 1887

GENUS *CIONA* FLEMING, 1822

***CIONA INTERMEDIA* MASTROTOTARO SP. NOV.**

lsid:urn:lsid:zoobank.org:act:362BF79A-E2A1-4B82-9CD9-FD8DE36CEAB9

*Type material*

*Holotype*: MUZAC-6550, 7 cm in height, July 2014, collected by F. Mastrototaro and G. Chimienti, type locality, 3–5 m depth, dissected, preserved in 5% formalin.

*Paratypes*: MUZAC-6551 and MUZAC-6552, two specimens preserved in 99% ethanol, collected by F. Mastrototaro and G. Chimienti, type locality, 3–5 m depth, not dissected. The holotype and the paratypes have been deposited in the collection of the Zoological Museum of the University of Bari.

*Type locality*: Olbia, north-eastern coasts of Sardinia, Italy (40°54'55"N, 9°34'05"E).

*Etymology*

The specific name refers to anatomical features of this species that appear intermediate compared with other species of *Ciona* (from Latin *inter*, between, and *medium*, middle).

*Morphological description*

Smooth and soft tunic, semi-transparent, without tubercular prominences. The inner part of the animal is visible and characterized by a reddish anterior region. The red pigmentation is attributable to the

red–orange spots present in the anterior part of the body wall, which become intensely red near the siphons (Figs 1A–C, 2A–C). In living specimens, the tunic does not follow the body during sudden contractions (Fig. 1A, C).

The oral and the atrial siphons are almost the same length (Fig. 2A, B), with the oral one being slightly longer. The oral aperture has eight lobes and the atrial has six (Fig. 2E). One red–orange ocellus lies between each lobe (Fig. 2F). At the base of the oral siphon there are ~30 narrow tentacles of different length, the longest alternating with the shortest ones (Fig. 3A, B).

The ripe specimen sampled is ~7 cm in length with the tunic, 5 cm extracted from the tunic (Fig. 2A–C, 4A). The thoracic wall is characterized by a strong musculature that consists of a longitudinal system of six well-defined bands of muscles running from the basal attachment to the siphons (Figs 2C–E, 5B), while the circular system is composed by thin transverse strands, encircling the whole body and evident on both siphons (Fig. 2G).

On each side, the oral siphon is crossed by four bands of longitudinal muscles that reach the margin of the oral lobes, and the atrial siphon is supplied by the other two longitudinal bands (Fig. 2E). The prepharyngeal area (Fig. 3A) does not have papillae (Fig. 3B). The flat pharynx (Fig. 3H) occupies a wide part of the zooid, consisting of many longitudinal vessels and numerous stigmata (Fig. 3F). The stigmata are crossed by narrow parastigmatic vessels (Fig. 3F). At each intersection between transverse vessels and longitudinal vessels is placed a ventrally notched papilla (Fig. 3G).

In the observed specimens, the number of longitudinal vessels on each side of the pharynx is 36, and the number of stigmata per mesh in the middle portion of the animal is four (Fig. 3E); these characters are considered not fixed, but variable with the size of the specimens in the other known *Ciona* species (Millar, 1953; Kott, 1990). No difference is noted in the meshes of the anterior and posterior part of the pharynx. The dorsal lamina is divided into numerous languets corresponding to the transverse vessels (Fig. 3D), with the endostylar appendix placed at its end (Fig. 3C).

The digestive system occupies about one-quarter of the whole size of the zooid, at its posterior end (Fig. 4A). The wide stomach is ovoid in shape and lies on the left side of the zooid. In particular, it is positioned slightly to the right of the mid-line, beneath the pharynx. In living specimens, the alimentary canal is clearly visible, with the orange stomach having ~40 irregular, broken folds on its surface (Fig. 4A, B). The intestine ends with a lobed anus that opens at the level of one-third of the upper part of the pharynx (Fig. 4A). The rectum is less long than the gonoducts (Fig. 4C).

The ovary, containing a large number of brown–yellowish oocytes ~100 µm in diameter (Figs 4C, D, 6A<sub>1</sub>),

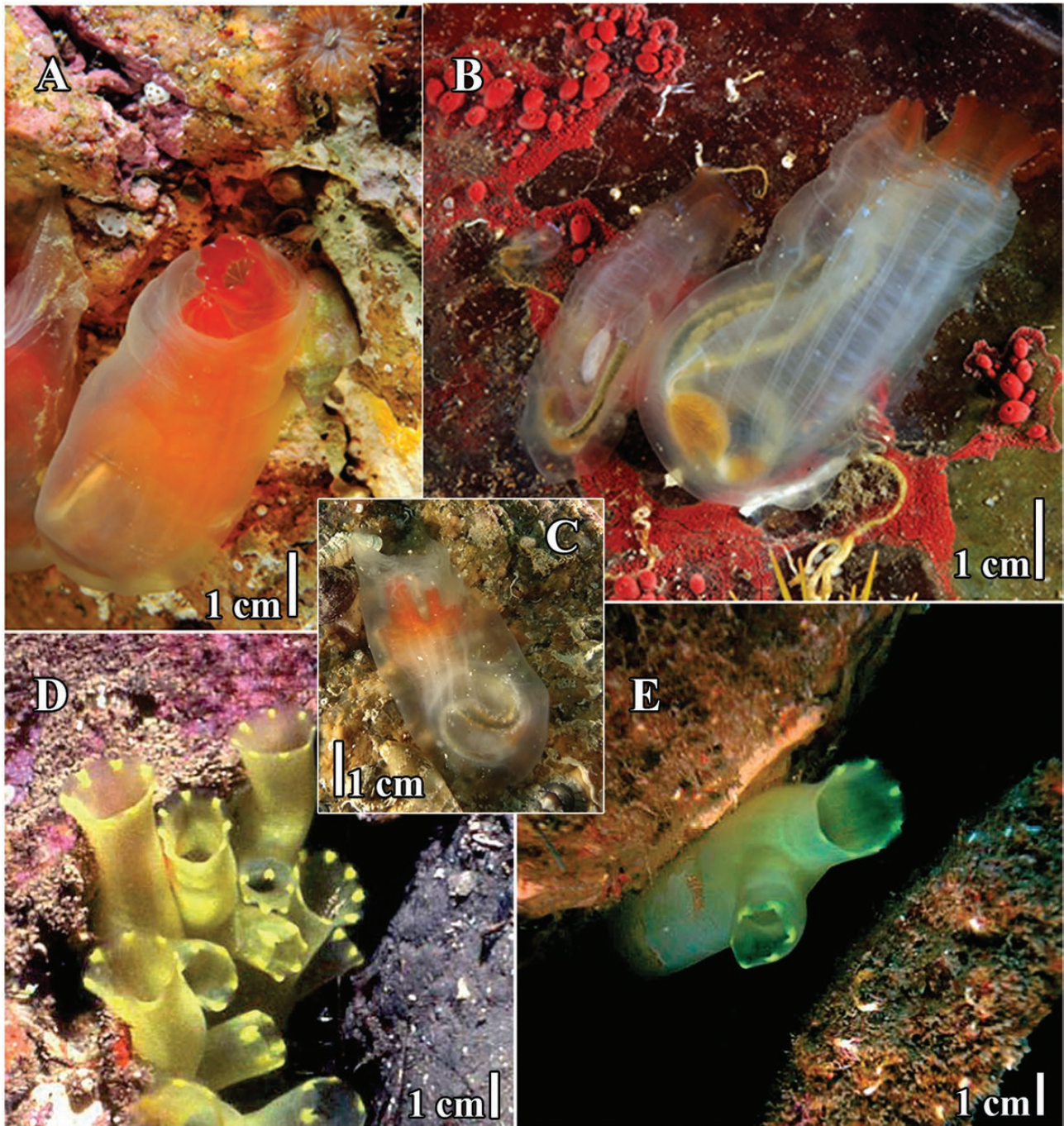


**Figure 1.** A–C, several living specimens of *Ciona intermedia* photographed and collected along the coasts of Olbia (Sardinia, Tyrrhenian Sea, Italy). D, E, living specimens of *Ciona edwardsi*, with the typical sulphur-yellow appearance, photographed along Ligurian coasts (Mastrototaro & Relini, 2011).

is positioned in the inner part of the sinusoidal loop formed by the gut. The oviduct extends parallel to the rectum, projecting beyond the anus, with the spermiduct running laterally to it (Fig. 4C). The walls and the end of the gonoducts are yellow–orange. The spermiduct is visible because of the accumulation of

white sperm (Fig. 4C), with four to eight white, narrow papillae projecting from its distal end (four papillae visible in Figs 4E, 6A). The branching system of tubular follicles forming the testis lies on both the stomach and the intestine, forming two major ducts, which join at the level of the ovary (Fig. 4F); this single spermiduct

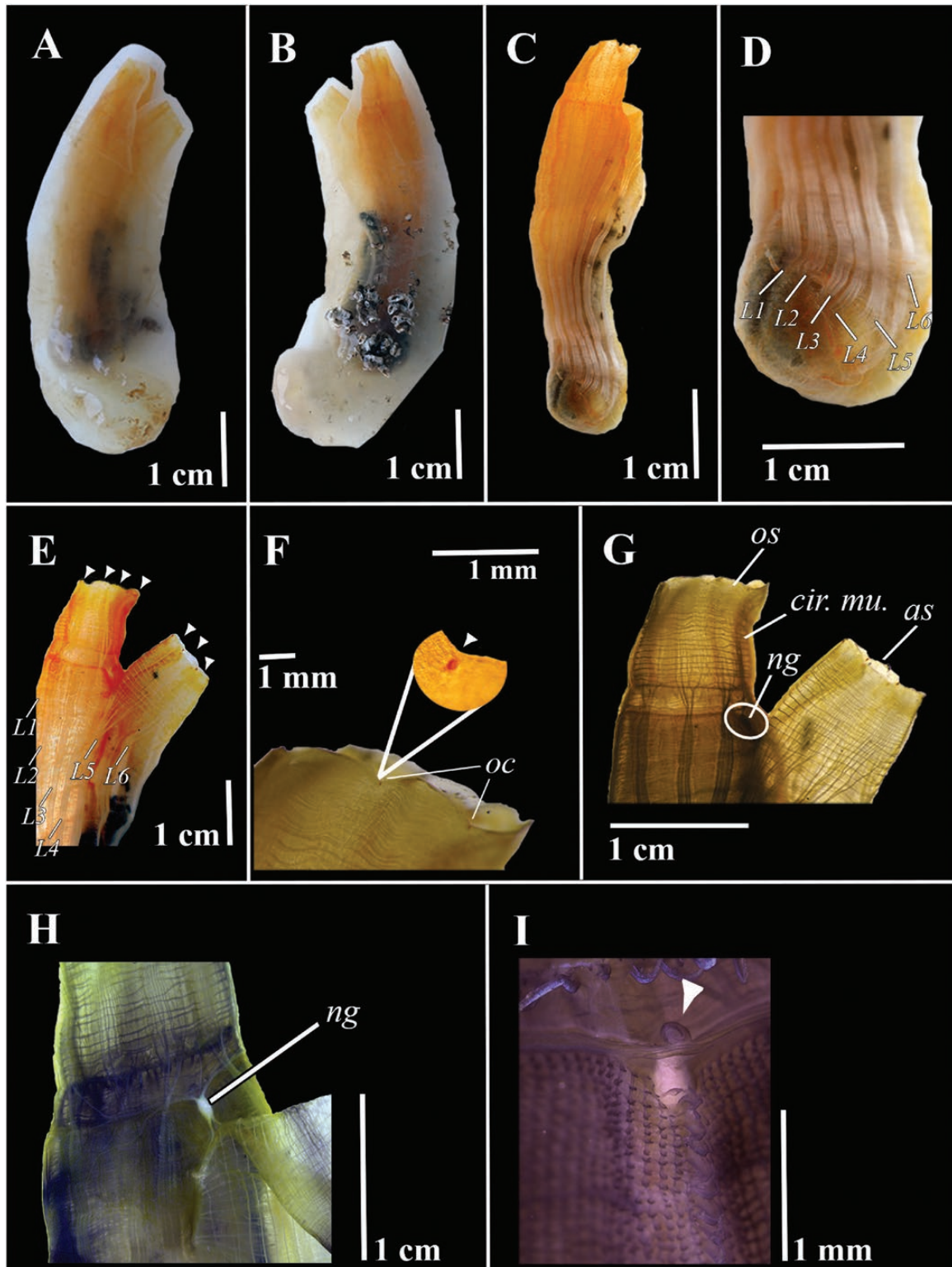


**Figure 2.** *Ciona intermedia*. A, left side of a specimen with the tunic. B, right side of a specimen with the tunic. C, specimen without the tunic, showing the six longitudinal muscle bands. D, magnification of the base of a specimen. White bars indicate the six longitudinal muscle bands (L1–L6). E, oral and atrial siphons with eight and six lobes, respectively (white arrowheads), and longitudinal muscle bands at the level of the siphons (L1–L6). F, red ocelli at the base between



runs parallel to the oviduct up to the genital aperture (Fig. 4C).

#### MOLECULAR PHYLOGENETIC RECONSTRUCTION

The percentage identity between *C. intermedia* and other *Ciona* species, including *C. roulei* and *C. edwardsi*, is lower than 94.28% for *cox1*, 90.14% for *x3n1* and 91.89% for *x2cb*. The *cox1* value is distant from the 2–3% divergence found in several taxonomic groups as the maximum *cox1* intraspecific divergence (Hebert *et al.*, 2003, 2004; Smith *et al.*, 2005), thus providing a first clue that *C. intermedia* could not belong to any *Ciona* species already subjected to molecular characterization (i.e. *C. intestinalis sensu Brunetti et al.*, 2015, *C. robusta*, *C. savignyi*, *C. roulei*, *C. edwardsi*, *Ciona* sp. C and *Ciona* sp. D).

Figure 7 summarizes the results of the species delimitation analyses and the phylogenetic reconstructions carried out on *cox1*. The bPTP method consistently identifies *C. intermedia* as a distinct OTU, using both BI and ML trees as input (see bPTP-Btree and bPTP-MLtree bars, respectively, in Fig. 7). The other recognized OTUs correspond to species already described (*C. edwardsi*, *C. robusta* and *C. savignyi*), to a species so far defined only by molecular characterization (*C. sp. D*) and to the cluster including *C. intestinalis* and *C. roulei* (Fig. 7). Contrary to expectation, *C. sp. C* is not recognized as a single OTU, but as two or three OTUs depending on the input tree (see differences between the bPTP-Btree and bPTP-MLtree bars in Fig. 7). The ABGD results demonstrate the existence of the barcode gap and show a perfect match between the initial and the recursive partitions for prior intraspecific divergences ranging from 0.10–0.28 (depending on the alignment used and parameter options) to 5.99% (see Supporting Information, Table S5). The results of the 72 (i.e. 18 × 4) ABGD analyses confirm the OTUs identified by bPTP, except for *C. sp. C* and few sporadic inconsistencies (Fig. 7; Supporting Information, Table S5). Indeed, *C. sp. C* is recognized as a single OTU in all ABGD analyses, except for a few partitions obtained with  $X = 1$ , where other species are also split incongruously in several improbable OTUs (see red values in square brackets in Supporting Information, Table S5).

*Ciona intermedia* is recognized as a single OTU in all ABGD analyses except in one case. It is merged with *C. edwardsi* into a single OTU only in the initial and recursive partitions corresponding to a prior

intraspecific divergence of 2.15%, obtained in the ABGD performed on the 1566-All alignment using the p-dist (see Supporting Information, Table S5). Going into the details of the 72 ABGD results (Supporting Information, Table S5), the 18 analyses performed on the same alignment with different parameters/substitution models give identical results, with only a few exceptions, mainly when using the p-dist (see 1566-All and 737-Nogap-47taxa alignments) or at the lowest prior intraspecific divergences for  $X = 1$ , especially in the alignment with the lowest site number (see square brackets values for the 451-Nogap-All alignment in Supporting Information, Table S5). Even the results of the ABGD analyses performed on the four different *cox1* alignments (i.e. 1566-All, 451-Nogap-All, 737-Nogap-47taxa and 1084-12taxa) are almost identical, because they identify OTUs with the same composition, except for some recursive partitions at the lowest prior intraspecific divergences for  $X = 1$  (see square brackets values in Supporting Information, Table S5). Remarkably, the 737-Nogap-47taxa and 1084-12taxa alignments give almost identical results in spite of the different species representativeness (at least three sequences for most species in the 737-Nogap-47taxa alignment; only one or two sequences per species in the 1084-12taxa alignment). All these results indicate that, at least for our *cox1* dataset, the ABGD method is robust to parameter variation, presence of missing data and differences in species representativeness, thus making us confident on the results obtained.

Remarkably, the OTUs identified by the bPTP and ABGD analyses on *cox1* correspond to clades strongly supported in the *cox1* phylogenetic trees (Fig. 7). Indeed, the bPTP/ABGD OTUs consisting of more than one specimen form statistically significant clades that have both ML bootstrap support  $\geq 90\%$  and BPP  $\geq 0.99$  (black dots in Fig. 7). Even the OTU mixing *C. roulei* and *C. intestinalis* sequences is identified as a well-supported clade (ML bootstrap, 95% and BPP, 1). It is noteworthy that *C. intermedia* forms the sister group of *C. edwardsi*, and this relationship is again strongly supported (ML bootstrap, 99% and BPP, 1; Fig. 7). Unfortunately, the basal nodes of Figure 7 remain unresolved. Therefore, our COI-1.2kb fragment is able to discriminate different *Ciona* species, demonstrating it to be a robust DNA barcode for the *Ciona* genus, but it is unable to clarify the exact phylogenetic relationships among the species.

The species delimitation analyses and the ML/Bayesian phylogenetic reconstructions based on the

each lobe, with the magnification of one red ocellus (white arrowhead). G, oral and atrial siphons, with circular muscle systems and the neural ganglion encircled in white. H, neural ganglion lying at the base of the oral and atrial siphons. I, magnification of the anterior region with dorsal tubercle (white arrowhead). Abbreviations: as, atrial siphon; cir. mu., circular muscles; ng, neural ganglion; oc, ocellus; os, oral siphon.

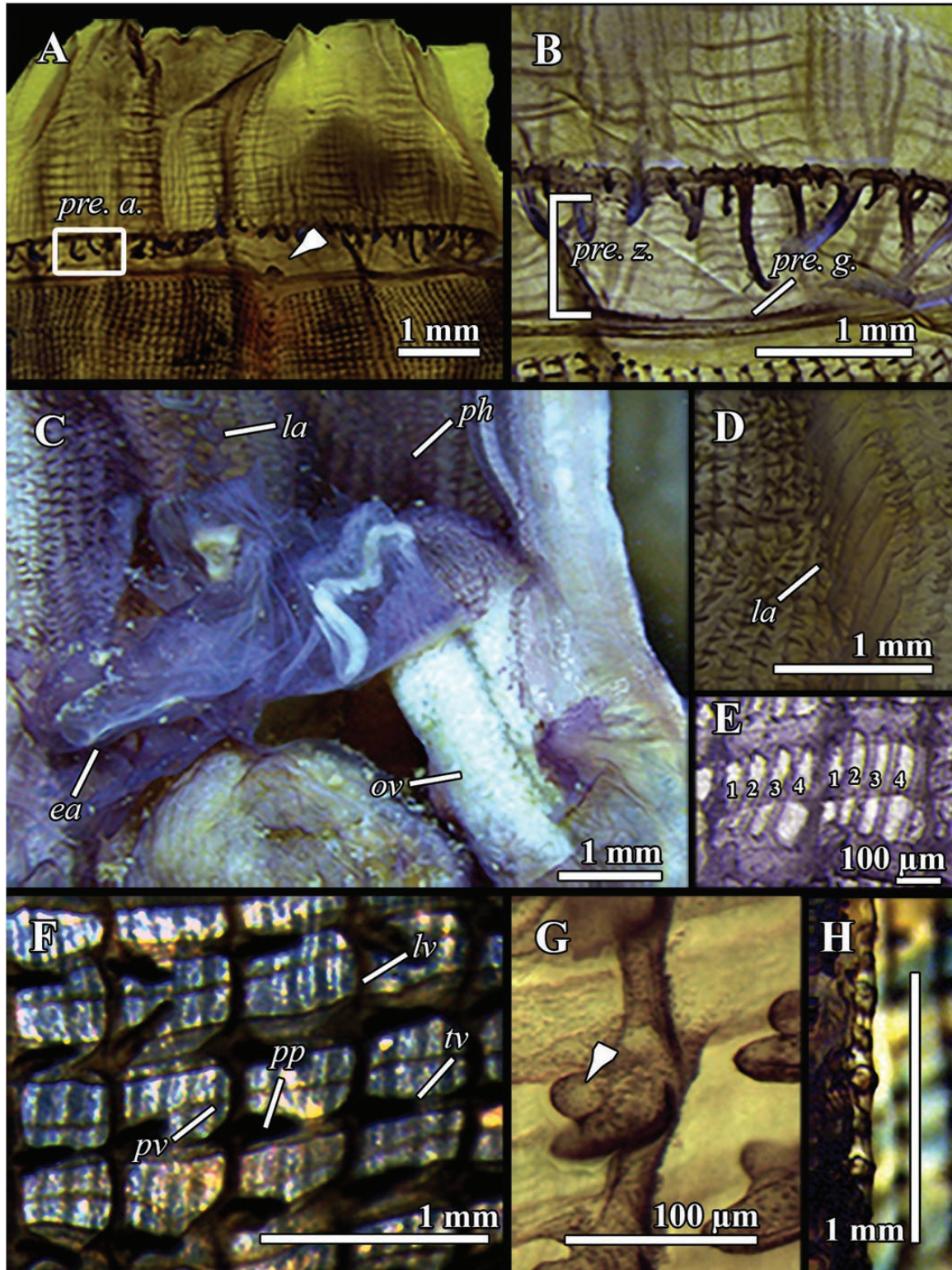


**Figure 3.** *Ciona intermedia*. A, prepharyngeal area (pre. a.). The white arrowhead indicates the dorsal tubercle. B, magnification of the prepharyngeal area, with a wide prepharyngeal zone (pre. z.) and a narrow prepharyngeal groove (pre. g.). Oral tentacles are clearly visible. C, bottom of the pharynx of a dissected specimen. D, dorsal lamina, with languets. E, magnification of the mesh of stigmata, with four stigmata per mesh (1–4). F, magnification of the branchial wall, with

x3n1 fragment (Fig. 8) confirm the results obtained with *cox1* (Fig. 7). Indeed, the bPTPs based on both the ML and the Bayesian trees give identical results and discriminate six OTUs, corresponding to: *C. intermedia*, two already described species (*C. edwardsi* and *C. robusta*), two molecularly identified cryptic species (*C. sp. C* and *C. sp. D*) and a clade consisting of *C. intestinalis* plus *C. roulei* (Fig. 8). The ABGD analyses indicate the existence of a clear barcode gap and show a perfect match between initial and recursive partitions at prior intraspecific divergences ranging from 0.77–1.29 (depending on distance metric) to 5.99% (see Supporting Information, Table S5). The results of the 18 ABGD analyses performed with different parameters/substitution models are mainly congruent (Supporting Information, Table S5) and identical to bPTP (Fig. 8). A few differences are observed only in the recursive partitions at the lowest intraspecific divergence (where *C. roulei* is recognized as a distinct OTU; see dashed bars in Fig. 8) and at a prior intraspecific divergence of 0.77–1.29% when using the p-dist, where *C. intermedia* is clustered with *C. edwardsi* in the same OTU (see red values in Supporting Information, Table S5). The x3n1 phylogenetic reconstructions recognize as highly supported: the sister relationship between *C. intermedia* and *C. edwardsi* (maximum bootstrap and BPP values), two clades corresponding to single species (i.e. *C. sp. D*, *C. robusta*) and the clustering of *C. intestinalis* with *C. roulei* (see black dots in Fig. 8). The sister relationship of *C. sp. C* to the *C. intermedia*–*C. edwardsi* clade obtains only marginal support (ML bootstrap, 57%; BPP, 0.91); therefore, it needs to be confirmed by additional data. Like *cox1*, x3n1 leaves unresolved the basal nodes of the *Ciona* tree. Figure 8 also reports the internal structure of the x3n1 mitochondrial fragment, highlighting that the gene order *cox3–trnK–nad1* is conserved in all reported *Ciona* species (except for *C. savignyi*; see Material and Methods). On the contrary, the length of the two non-coding spacers upstream and downstream of *trnK*, respectively, varies between species (see yellow and blue boxes in Fig. 8), thus causing the overall variability in size of the x3n1 fragment between species.

The x2cb fragment is ~1.1 kb long and is characterized by a short overlap between the open reading frames (ORFs) of the two genes in all three species (*C. edwardsi*, *C. intermedia* and *C. roulei*) analysed here for the first time. The same situation was found in all other published mt genomes of *Ciona*

species (see Supporting Information, Table S3). The ML and BI phylogenetic reconstructions based on this x2cb fragment are shown in Figure 9. Remarkably, all nodes of this phylogeny, including the basal ones, are fully resolved (ML bootstrap  $\geq 93\%$  and BPP  $\geq 0.97$ ; see black dots in Fig. 9), thus providing clear information about the relationships between the *Ciona* species. *Ciona intermedia* is confirmed as the sister clade of *C. edwardsi*, and *C. robusta* is the sister group of the cluster mixing *C. intestinalis* and *C. roulei*. Finally, *C. savignyi* is basal to the remaining *Ciona* species.

## DISCUSSION

The family Cionidae includes three genera, *Araneum*, *Ciona* and *Tantillulum*, characterized by solitary animals with a transparent tunic, the stomach positioned under the pharynx and the gonad lying in the gut loop (Brunetti & Mastrototaro, 2017). *Ciona* is typical of shallow waters, but the genus also includes some abyssal species (Brunetti & Mastrototaro, 2017), and *C. intestinalis* has even been found below 100 m deep in the Oslo Fjord (Dybern, 1967). *Ciona* can be distinguished by the presence of longitudinal and parastigmatic vessels with papillae in the pharynx, oral and atrial siphons, with eight to ten and six to eight lobes, respectively, and the presence of ocelli between the lobes. In some species, the endostyle ends with an appendix, and the stomach lies on the left side of the zooid (Millar, 1953; Brunetti & Mastrototaro, 2017). Some characteristics of the papillae projecting from the spermiduct (i.e. shape, number and pigmentation) and the oocyte size have been used as further features to allow specific identification. In particular, these characters have been described previously in four *Ciona* species (Hoshino & Nishikawa, 1985; Caputi *et al.*, 2007; Sato *et al.*, 2012; supplementary material in the study by Malfant *et al.*, 2018; Fig. 6).

The morphological and ecological traits of the specimens described in the present study confirm that they belong to the genus *Ciona* but do not fit into any of the described *Ciona* species reported so far in the Mediterranean and in other seas. In the genus *Ciona*, 15 species are currently valid and briefly described below: *Ciona antarctica* Hartmeyer, 1911, *C. edwardsi*, *Ciona fascicularis* Hancock, 1870, *Ciona gelatinosa* Bonnevie, 1896, *Ciona hoshinoi* Monniot, 1991, *Ciona imperfecta* Monniot & Monniot, 1977, *C. intermedia*,

the papillae placed at the intersection between the transverse vessels and the longitudinal vessels. Stigmata are crossed by a narrow parastigmatic vessel. G, magnification of the papillae. White arrowhead indicates the notch. H, section of the flat branchial wall. Abbreviations: ea, endostylar appendix; la, languet; lv, longitudinal vessel; ov, ovary; ph, pharynx; pp, papilla; pre. a., prepharyngeal area; pre. g., prepharyngeal groove; pre. z., prepharyngeal zone; pv, parastigmatic vessel; tv, transverse vessel.

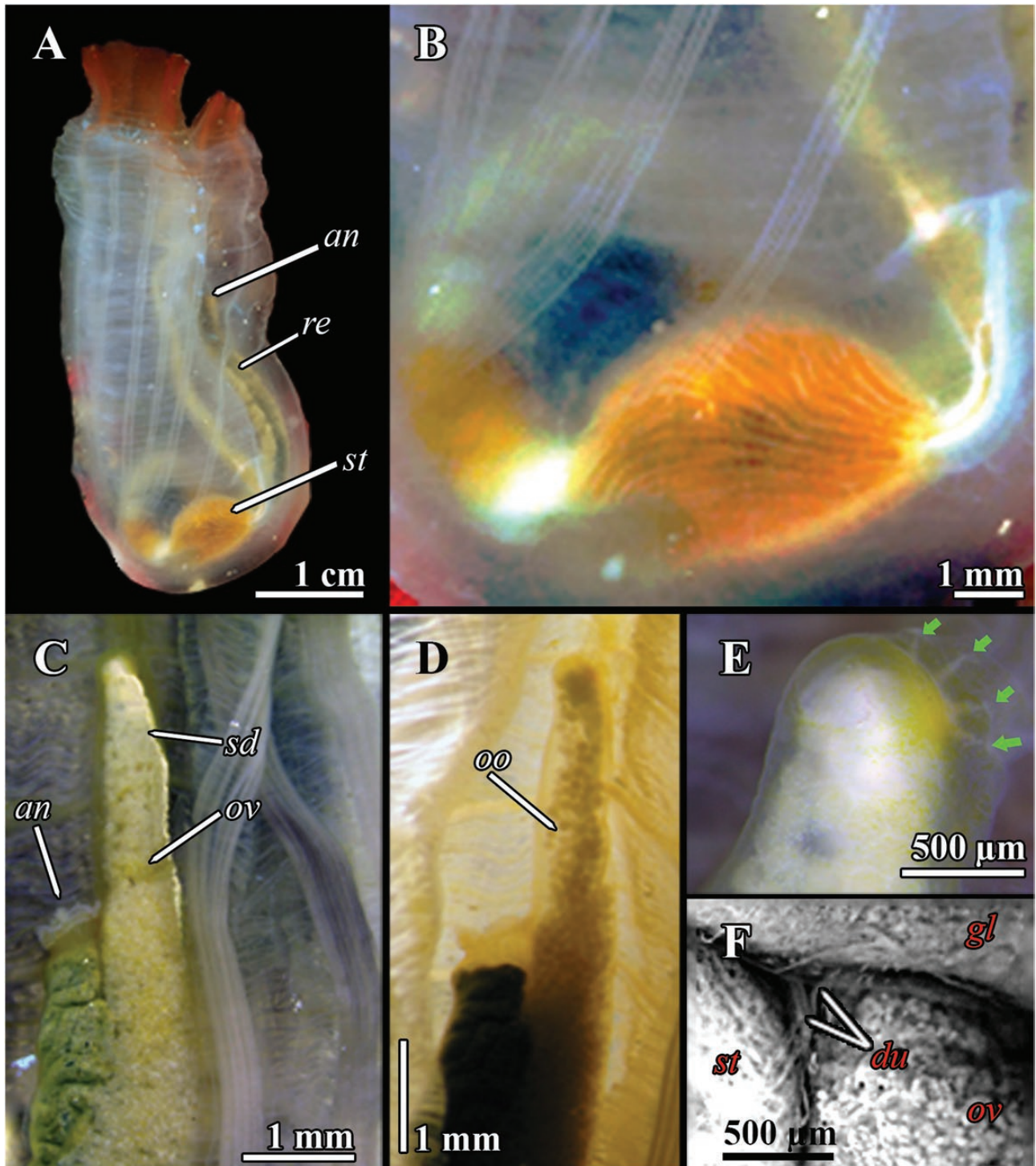


**Figure 4.** *Ciona intermedia*. A, living specimen, with orange stomach. B, stomach with ~40 irregular broken folds on its surface. C, high magnification of the ovary and lobed anus. D, ovary, with numerous oocytes. E, high magnification of the end of the gonoduct apertures, showing the orange–yellow pigments and the four visible papillae at the distal end of the spermiduct (green arrows). F, high magnification of the abdominal region, showing testis follicles between the stomach and the posterior gut loop forming two ducts that join into a single spermiduct at the level of the ovary. Abbreviations: an, anus; du, collecting ducts of the testis; gl, gut loop; oo, oocytes; ov, ovary; re, rectum; sd, spermiduct; st, stomach.

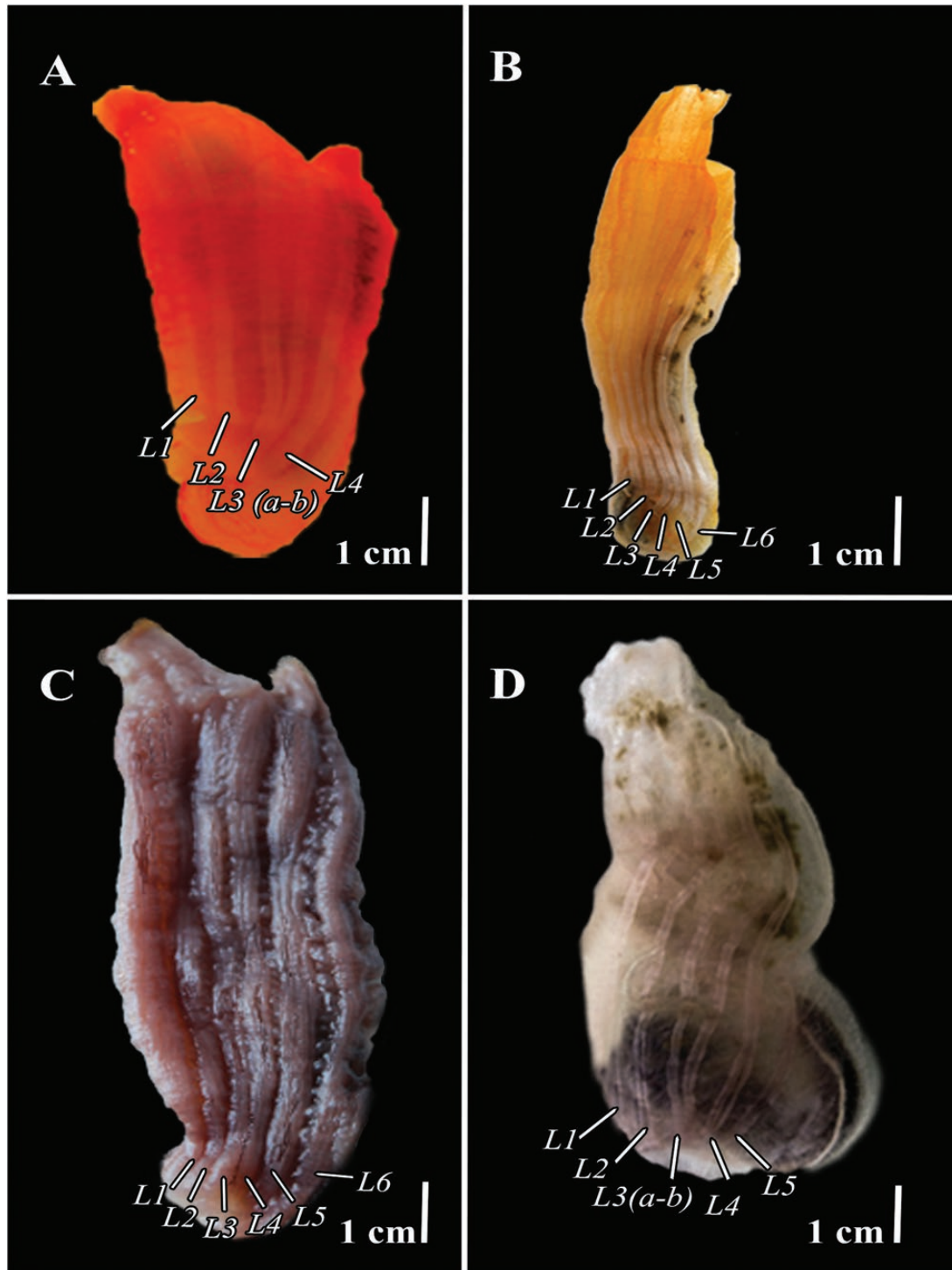


**Figure 5.** Comparison of four *Ciona* species, with white lines highlighting the number of muscle bands (L1–L6; “L3 a–b” indicates that the third muscle band could be divided in two bands). A, *Ciona roulei* (courtesy of Marie Nydam). B, *Ciona intermedia* collected in Olbia (Sardinia, Italy). C, *Ciona edwardsi* collected in Sorrento, Tyrrhenian Sea by F. Mastrototaro. D, *Ciona robusta* collected along the coasts of Taranto, Ionian Sea (Mastrototaro *et al.*, 2008).

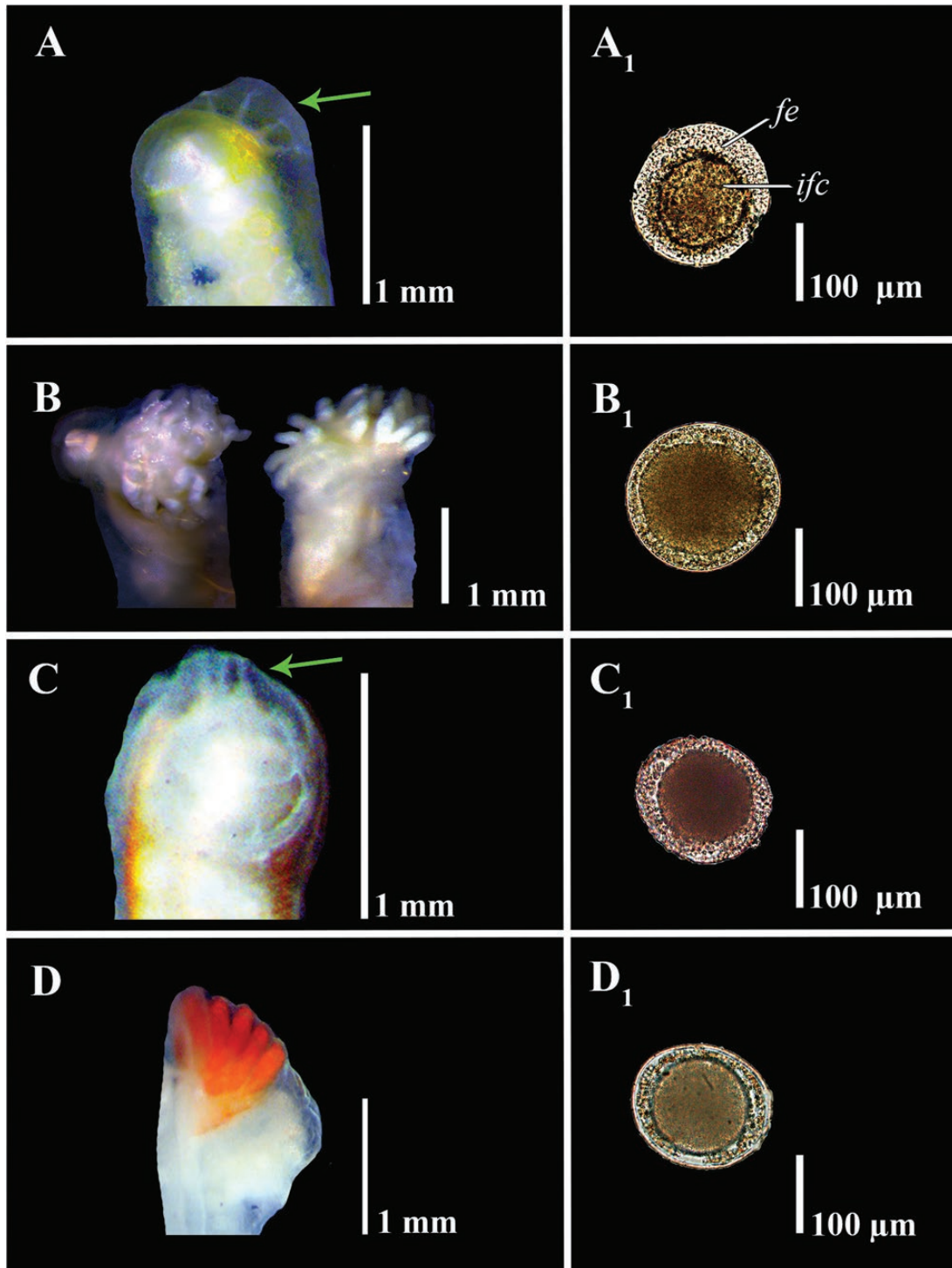


**Figure 6.** Comparison between spermiduct ends and oocytes of four *Ciona* species. A, A<sub>1</sub>, *Ciona intermedia*, spermiduct with four visible papillae (green arrow), oocyte ~100 μm in diameter and a large outer follicular envelope. B, B<sub>1</sub>, *Ciona edwardsi*, lateral and back view of the spermiduct with numerous papillae and oocyte larger in size than the oocytes found in the other three species. C, C<sub>1</sub>, *Ciona intestinalis*, spermiduct with white papillae (green arrow) and oocyte ~100 μm in diameter. D, D<sub>1</sub>, *Ciona robusta*, spermiduct with ellipsoidal red papillae and oocyte ~100 μm in diameter. Abbreviations: fe, follicular envelope; ifc, inner follicle cells.

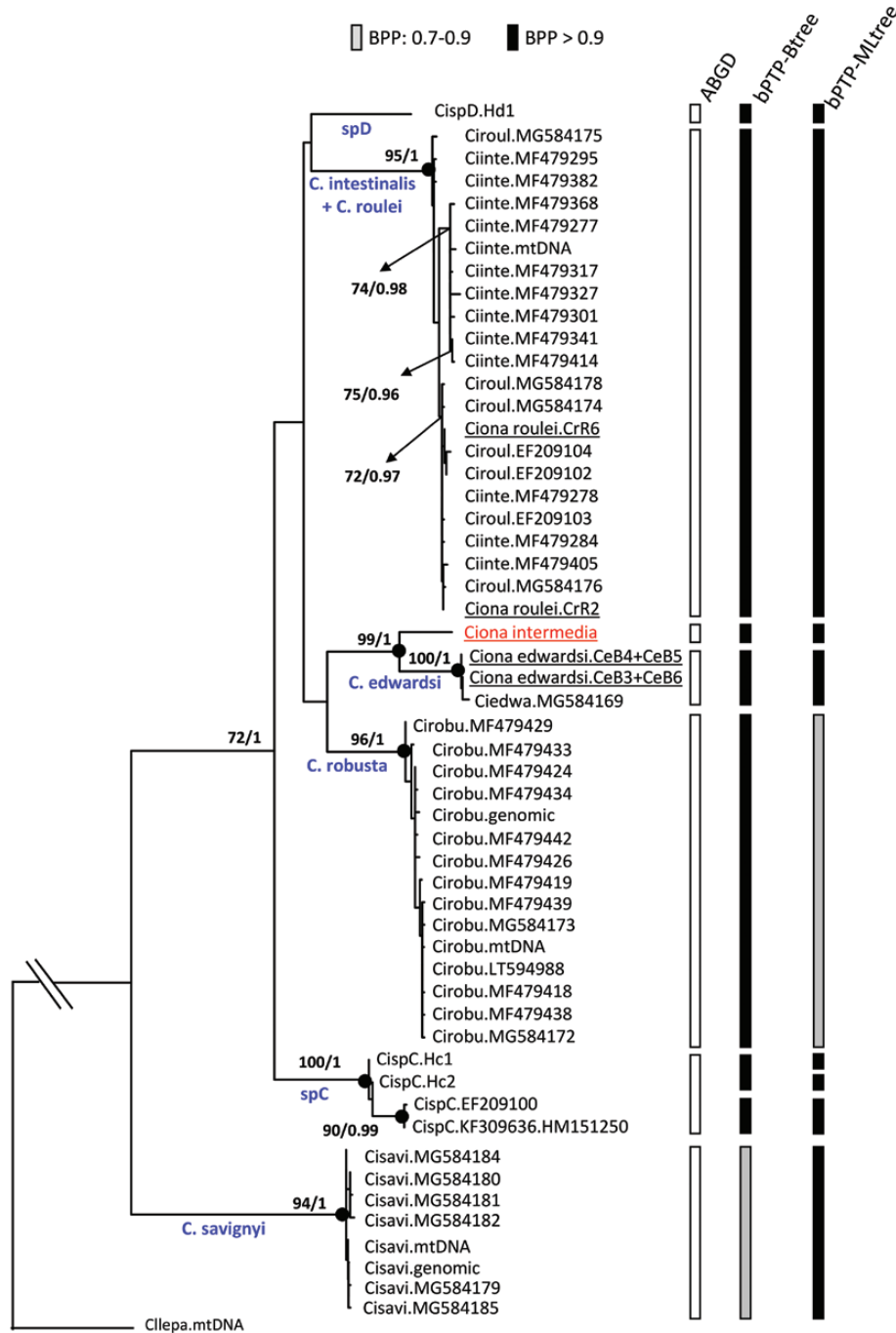


**Figure 7.** Maximum likelihood tree based on the COI-1.2kb fragment, with mapping of the OTUs identified by the ABGD and bPTP analyses (vertical bars). Branch length is proportional to the number of substitutions per sites. Values close to the nodes are ML bootstrap percentage/BPP and are shown only when both bootstrap  $\geq 70\%$  and BPP  $\geq 0.90$ . Black dots are nodes having both bootstrap support  $\geq 90\%$  and BPP  $\geq 0.99$ . Underlining indicates sequences obtained in the present study. *Clavelina lepadiformis* (Cllepa.mtDNA) was used as the outgroup. Abbreviations: ABGD (automatic barcode gap discovery) indicates OTUs consistently identified by the 72 ABGD analyses detailed in the [Supporting Information \(Table S5\)](#); BPP, Bayesian posterior probability; bPTP, Bayesian implementation of the PTP; bPTP-Btree, bPTP performed on the Bayesian tree; bPTP-MLtree, bPTP performed on the ML tree; Ciedwa, *Ciona edwardsi*; Ciinte, *Ciona intestinalis*; Cirobu, *Ciona robusta*; Ciroul, *Ciona roulei*; Cisavi, *Ciona savignyi*; CispC, *Ciona* sp. C; CispD, *Ciona* sp. D; ML, maximum likelihood; OTU, operational taxonomic unit. Analysed sequences are listed in the [Supporting Information \(Table S2\)](#).

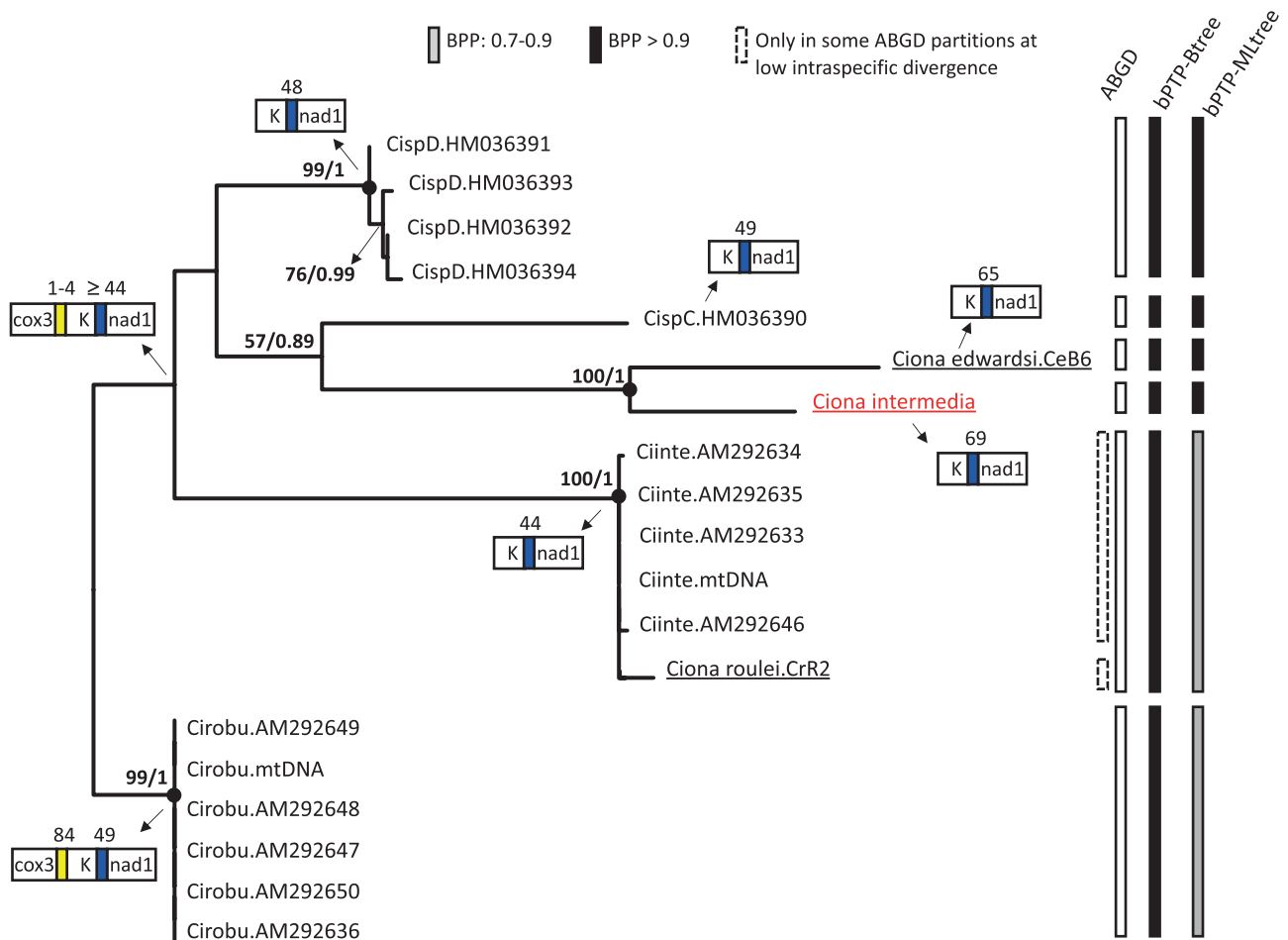


**Figure 8.** Maximum likelihood tree based on the x3n1 fragment, with diagram of the gene content of the x3n1 fragment and mapping of the OTUs identified by ABGD and bPTP analyses (vertical bars). Branch length is proportional to the number of substitutions per sites. Values close to the nodes are the maximum likelihood bootstrap percentage/BPP and are reported only when > 50/0.50. Blue and yellow boxes in the gene content diagram indicate non-coding spacers, with length in base pairs. Black dots indicate nodes having both bootstrap support  $\geq 90\%$  and BPP > 0.99. Underlining indicates sequences obtained in the present study. Abbreviations: ABGD (automatic barcode gap discovery) indicates OTUs identified by the 18 ABGD analyses detailed in the [Supporting Information \(Table S5\)](#), with dashed bars indicating some recursive partitions at the lowest intraspecific divergence; BPP, Bayesian posterior probability; bPTP, Bayesian implementation of the PTP; bPTP-Btree, bPTP performed on the Bayesian tree; bPTP-MLtree, bPTP performed on the maximum likelihood tree; K, *trnK* gene. Species codes are as in [Figure 7](#). Analysed sequences are listed in the [Supporting Information \(Table S4\)](#).

*C. intestinalis*, *Ciona longissima* Hartmeyer, 1899, *Ciona mollis* Ritter, 1907, *Ciona pomponiae* Monniot & Monniot, 1989, *C. robusta*, *C. roulei*, *C. savignyi* and *Ciona sheikoi* Sanamyan, 1998.

*Ciona antarctica* is rarely collected and known only from Antarctic waters between 300 and 500 m deep (Hartmeyer, 1911; Monniot & Monniot, 1983; Ramos-Esplá *et al.*, 2005; Monniot *et al.*, 2011). This species is characterized by the gonoducts ending before the anus and by a peculiar organ of unknown function on each side of the posterior part of the body, between the gut and the body wall, made up of thick-lobed lamellae (Monniot, 1998).

*Ciona gelatinosa*, known from the Arctic, North Atlantic (Van Name, 1945; Hoshino & Nishikawa, 1985) and north-eastern Pacific (Sanamyan & Sanamyan, 2007), is characterized by the gonoducts ending before the anus and by a large muscular post-abdominal extension of the body wall, no endostylar appendix and the absence of pigment spots around the male papillae or on other parts of the body (Sanamyan & Sanamyan, 2007).

*Ciona fascicularis* has been recorded mainly along the north-western Atlantic coasts and presents peculiar cylindrical rhizoids at the base of the body (Hancock, 1870; Monniot, 1963).



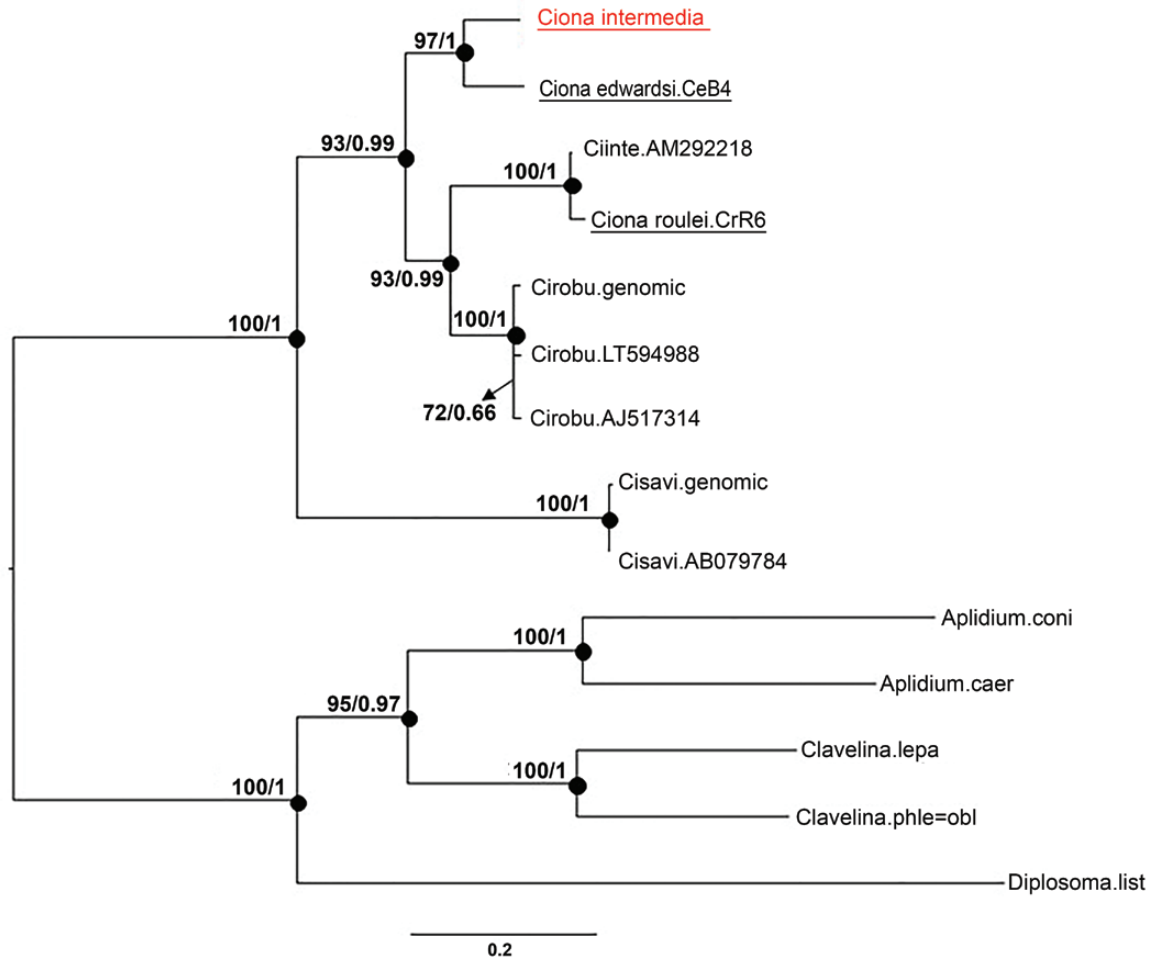


**Figure 9.** Maximum likelihood based on the x2cb fragment, consisting of the partial sequences of the *cox2* and *cob* genes. Branch length is proportional to the number of substitutions per sites. Values close to the nodes are the maximum likelihood bootstrap percentage/Bayesian posterior probability. Black dots indicate nodes having both bootstrap support  $\geq 90\%$  and Bayesian posterior probability  $\geq 0.99$ . Underlining indicates sequences obtained in this study. Five Aplousobranchia species were used as outgroups: *Aplidium conicum* (*Aplidium.coni*), *Aplidium coeruleum* (*Aplidium.caer*), *Diplosoma listerianum* (*Diplosoma.list*), *Clavelina lepadiformis* (*Clavelina.lepa*) and *Clavelina phlegraea*, a junior synonym of *Clavelina oblonga* (*Clavelina.phle = obl*) (Ordóñez *et al.*, 2016). Other species codes are as in Figure 7. Analysed sequences are listed in the Supporting Information (Table S3).

*Ciona hoshinoi* is known from a single specimen from New Caledonia and another one collected in Palau, both 1.5 cm in length, with the Palau specimen being extremely contracted (Monniot, 1991; Monniot & Monniot, 2001). This species is characterized mainly by the presence of small, round papillae between transverse vessels and longitudinal vessels and by smaller papillae associated only with the parastigmatic vessels, in addition to a smooth stomach and an anus ending at the level of the aperture of the gonoducts (Monniot, 1991).

*Ciona imperfecta* is an abyssal species recorded at 4000 m depth. It lacks the endostylar appendix and has a pharynx consisting of only four rows of stigmata

and five or six longitudinal vessels (Brunetti & Mastrototaro, 2017).

*Ciona longissima* has a peculiar long stalk at the base of its body and has been recorded only in Arctic waters deeper than 1000 m.

*Ciona mollis* was collected for the first time by Ritter in 1907 off California at 2000 m depth and in the Mexican Pacific at 4400 m depth (Monniot, 1998). The musculature of this species is unusual; six strong muscular bands on each side converge to a round area along the ventral side, with the bands stopping at the end of this area. It has a bilobed anus ending near the aperture of the gonoducts. The spermiduct is characterized by only one papilla, and

it has no endostylar appendix and no transverse body muscles.

*Ciona pomponiae* was based originally on only one specimen collected at a depth between 300 and 800 m off the Galapagos Islands (Monniot & Monniot, 1989) and it was subsequently recorded in the north-eastern Pacific (Sanamyan & Sanamyan, 2007) and from the Bering Sea as *Ciona gefesti* Sanamyan, 1998 (synonymized with *C. pomponiae* by Sanamyan & Sanamyan, 2007). *Ciona pomponiae* has only four longitudinal muscle bands, and a poorly defined stomach with folds, not clearly distinct from the intestine (Sanamyan & Sanamyan, 2007).

The description of *C. sheikoi* is based on 12 specimens recorded in the north-western Pacific region, all characterized by thick longitudinal mantle muscles, long and remarkably curved gonads and well-defined, cylindrical lobes around the anus. This species presents papillae on the enlarged posterior part of the tunic, no endostylar appendix and a smooth stomach, with the anus placed near the openings of the gonoducts (Sanamyan, 1998).

Each of the species above has peculiarities that prevent their possible misidentification as *C. intermedia*. The remaining five species are currently known in the Mediterranean Sea. *Ciona intestinalis* and *C. robusta* are both characterized by a pleated branchial wall (like an accordion), five or six longitudinal muscles (usually five, with the third divided into two bands) and transverse vessels of different sizes. *Ciona robusta* can also be distinguished from the similar *C. intestinalis* by the presence of several tubercles on the surface of the tunic, especially around the siphons, where they are usually arranged in longitudinal rows (Brunetti *et al.*, 2015).

*Ciona edwardsi* is typically found in shady sites and in circalittora-moderately deep waters, and has a bright sulphur-yellow coloration (Fig. 1D, E; Mastrototaro & Relini, 2011). At morphological level, this species is characterized by six longitudinal muscle bands (Fig. 5C) and by a pharynx with a flat branchial wall and transverse vessels of about equal sizes (Copello *et al.*, 1981; Mastrototaro *et al.*, 2000; Mastrototaro & Relini, 2011; Brunetti & Mastrototaro, 2017).

*Ciona roulei*, a poorly described species, is mainly characterized by the presence of four longitudinal muscle bands (with the third divided into two bands) and a reddish coloration (Lahille, 1890; Harant & Vernières, 1933; Brunetti & Mastrototaro, 2017). The validity of this species is still questionable, as suggested by the results of crossing experiments (Malfant *et al.*, 2018) and by molecular phylogenetic reconstructions of the *Ciona* genus based on both nuclear and mitochondrial genes (Nydam & Harrison, 2007, 2010; see tree in the study by Malfant *et al.*, 2018: fig. S1).

*Ciona savignyi*, first collected and described by Herdman (1882), is characterized by a whitish grey tunic, large paddle-shaped papillae on the intersection between transverse and longitudinal vessels and no endostylar appendix (Hoshino & Nishikawa, 1985; Brunetti & Mastrototaro, 2017). The presence of this species in the Mediterranean Sea is doubtful (Brunetti & Mastrototaro, 2017).

As summarized in Table 2, *C. intermedia* shows characters intermediate between those of the above-reported shallow-water *Ciona* species, i.e. a mixture of features, each one in common with only one or some of the other *Ciona* species. *Ciona intermedia* has been found in shady sites, as *C. edwardsi* (Table 2). It has six longitudinal muscle bands like all other species except for *C. roulei* (Fig. 5), a flat pharynx as in *C. edwardsi*, instead of the accordion-shaped pharynx of *C. intestinalis* and *C. robusta* (Fig. 3H), transverse vessels of about equal sizes, as in *C. edwardsi* and *C. roulei* (Brunetti & Mastrototaro, 2017), and a smooth tunic surface without the tubercles identified as a diagnostic feature of *C. robusta* by Brunetti *et al.* (2015; Table 2). *Ciona intermedia* appears morphologically similar to *C. edwardsi* (Table 2), but it has been found in shallower locations (i.e. littoral–shallow, at 3–5 m depth, whereas *C. edwardsi* is commonly present in circalittoral–moderately deep waters, at 20–40 m depth) and displays a different pigmentation. Although the coloration is generally not considered as a valid taxonomic character, it is important to point out that all *C. edwardsi* records show a characteristic sulphur-yellow coloration (Copello *et al.*, 1981; Mastrototaro *et al.*, 2000; Mastrototaro & Relini, 2011; Table 2). Concerning the number of papillae projecting from the spermiduct, the specimens of *C. intermedia* show from four to eight narrow colourless papillae at the distal end of the spermiduct (Fig. 6A), a situation more similar to that of *C. intestinalis* (Fig. 6C), whereas *C. edwardsi* shows a turf of 15–30 thick, white papillae projecting from all around the spermiduct, as reported by Hoshino & Nishikawa (1985; Fig. 6B; see also Table 2). *Ciona robusta* is characterized by ellipsoidal papillae, usually orange in colour, although their colour cannot be considered a true diagnostic character (Fig. 6G; see also *C. intestinalis* sp. A of Caputi *et al.*, 2007 and Sato *et al.*, 2012; Brunetti *et al.*, 2015; Malfant *et al.*, 2018). Finally, the diameter of oocytes of *C. edwardsi* is almost twice that of the other three species analysed, and they present a narrower follicular envelope (Fig. 6A<sub>1</sub>–D<sub>1</sub>). A larger size of the *C. edwardsi* oocytes has been also reported by Malfant *et al.* (2018) in comparison to *C. robusta*, *C. intestinalis* and *C. roulei*.

The examination of a larger number of *C. intermedia* specimens is needed for further verification of the intraspecific variability of the morphological traits

**Table 2.** Comparison of *Ciona intermedia* with the other four Mediterranean *Ciona* species

Characteristic	<i>Ciona intestinalis</i> *	<i>Ciona robusta</i> †	<i>Ciona roulei</i>	<i>Ciona edwardsi</i>	<i>Ciona intermedia</i>
Habitat‡	Light sites	Light sites	–	Shady sites	Shady sites
Colour <i>in vivo</i>	Various: whitish, reddish or yellowish	From whitish to yellowish	Red	Sulphur yellow	Transparent tunic; siphons and upper part of the body orange–red
Depth	Littoral, shallow water	Littoral, shallow water	Littoral, shallow water	Cirralittoral, moderately deep waters	Littoral, shallow water
Size (height; cm)	~20	~20	~10	~20	~7
Test surface	Smooth	With tubercles	Smooth	Smooth	Smooth
Number of oral lobes	8	8	–	8–10	8
Number of atrial lobes	6	6	–	6–8	6
Number of muscle bands (per side)§	5–6	5–6	4	5–6	6
Branchial wall	Pleated	Pleated	–	Flat	Flat
Transverse vessels (observed on the external surface)	Of different size	Of different size	Of about equal size	Of about equal size	Of about equal size
Spermiduct papillae	5–20, ellipsoidal, variable in colour, usually white	5–20, thick, variable in colour, usually orange–red	5–10, white	15–30, thick, white–yellow	4–8, narrow, white
Diameter of oocytes (µm)	~100	~100	~100	~200	~100

\*According to Brunetti *et al.*, (2015), formerly known as *Ciona intestinalis* type B.

†According to Brunetti *et al.*, (2015), formerly known as *C. intestinalis* type A.

‡Differences probably attributable to the different phototropism of the larvae (positive in *C. intestinalis* and *Ciona robusta*, probably negative in *Ciona edwardsi*; Brunetti & Mastrototaro, 2017)

§Variable character; the third band is sometimes divided into two bands.

investigated here and to search for character(s) unique to this species, if any.

With regard to the molecular data, the species delimitation analyses have been carried out with a clustering (ABGD) and a tree-based (bPTP) method on two molecular markers: COI-1.2kb (i.e. an elongation of the classical *cox1* DNA barcode) and x3n1. Both methods and markers consistently recognize *C. intermedia* as a distinct OTU and confirm that it cannot be assigned to any known described or undescribed *Ciona* species, including *C. sp. C* and *C. sp. D*, which are currently defined only by molecular data (Figs 7, 8). The congruency of these results increases the confidence in their validity. Indeed, the combined usage of two distinct methods/markers allows compensation for possible confounding factors differentially affecting the efficacy and/or sensitivity of each method/marker. With respect to the sample size and species representativeness, our datasets consist of at least three sequences for 50–70% of the expected species (for the x3n1 and *cox1* alignments, respectively), thus they are characterized by an uneven sampling similar to that observed in other species delimitation studies (for example, see Kekkonen & Hebert, 2014; Kekkonen *et al.*, 2015). Based on simulation tests (N. Puillandre, pers. comm.) and on the many studies that have used ABGD in combination with other methods, ABGD works well enough even when some species in the dataset include only one or two specimens (Kekkonen & Hebert, 2014; Kekkonen *et al.*, 2015; Ahrens *et al.*, 2016). Moreover, in our case, the unbalanced sampling is attributable to the fact that not only *C. intermedia*, but also *C. sp. C* and *C. sp. D* have been found and sampled in only one locality (Nydham & Harrison, 2007, 2010; Zhan *et al.*, 2010). Therefore, these three species belong to the so-called ‘singletons’, estimated to account for ~30% of formally described invertebrate species (Lim *et al.*, 2012). The commonness of rarity in nature and the consequent incomplete taxon sampling is a problem frequent in many DNA-based species delimitation studies (Lim *et al.*, 2012). However, recent analyses have shown that the shortcomings of poor and unbalanced sampling can be overcome by including data from related lineages (the so-called ‘subclade addition’), i.e. by extending the study of a focal clade to a broader set of species (Talavera *et al.*, 2013; Ahrens *et al.*, 2016). Ahrens *et al.* (2016) have also shown that this strategy has a different performance on the different species delimitation methods. In particular, in subclade analyses ABGD decreases, whereas PTP increases the number of recognized OTUs compared with the analysis of a total dataset consisting of all subclades, with consequent variation of the match to morphospecies (Ahrens *et al.*, 2016). Here, in order to at least mitigate the singleton issue in our datasets, we have analysed the sequences of all available

*Ciona* species with the two methods, ABGD and PTP, that were shown to be affected differently by the uneven sampling and to have a different response to the subclade addition strategy (Ahrens *et al.*, 2016). Nevertheless, both ABGD and PTP methods give consistent results, including the identification of *C. intermedia* as a distinct species.

*Ciona intermedia* is identified as the sister group of *C. edwardsi* with high statistical support in all ML and BI phylogenetic reconstructions based on all three analysed mt fragments (Figs 7–9), thus corroborating the close similarity already observed at the morphological level. Interestingly, interspecific crosses between *C. edwardsi* and any of the three species *C. intestinalis*, *C. robusta* and *C. roulei* revealed strong reproductive isolation (Lambert *et al.*, 1990; Malfant *et al.*, 2018). Therefore, given the strong genetic similarity between *C. intermedia* and *C. edwardsi*, we can hypothesize that *C. intermedia* might also be isolated reproductively from other *Ciona* species. Of course, this hypothesis needs to be tested experimentally. The use of nuclear markers could also be helpful to delineate these two species better and to investigate their past demographic history, as was done for *C. intestinalis* and *C. robusta* (Roux *et al.*, 2013; Bouchemousse *et al.*, 2016c).

Finally, the phylogeny of the genus *Ciona* inferred from x2cb gives, for the first time, a well-resolved picture of the relationships within this genus, even at the basal level (Fig. 9). Indeed, the basal nodes of the *Ciona* tree are unresolved in all previously published phylogenetic reconstructions of this genus, which were based on a *cox1* fragment of only 750 bp (Nydham & Harrison, 2007; Malfant *et al.*, 2018), on nuclear genes (Nydham & Harrison, 2010) or on combined nuclear and mt sequences (Zhan *et al.*, 2010). It is noteworthy that these previous phylogenetic reconstructions do not include one or two of the following *Ciona* species that have rarely undergone molecular sampling: *C. sp. C*, *C. sp. D* and *C. edwardsi* (absence of *C. sp. D* in the study by Nydam & Harrison, 2007, 2010; absence of *C. edwardsi* in the study by Zhan *et al.*, 2010; absence of *C. sp. C* and *C. sp. D* in the study by Malfant *et al.*, 2018); therefore, they analyse an incomplete species dataset, exactly like our x2cb tree. Thus, the better resolution observed in our x2cb phylogenetic tree cannot be an artefact related to the analysis of a reduced taxon sampling (i.e. lack of *C. sp. C* and *C. sp. D*). Furthermore, our results show that x2cb has a resolving power even higher than the *cox1* fragment of ~1.2 kb, because it is able to resolve all nodes that instead remain unresolved in our COI-1.2kb tree (compare Figs 7, 9). Moreover, even the COI-1.2kb ML and BI trees reconstructed using exactly the same taxon sampling of x2cb (i.e. excluding *C. sp. C* and *C. sp. D* from the *cox1* dataset) are not fully resolved

(data not shown), supporting the conclusion that the low resolution of *cox1* is not related to the presence of *C. sp. C* and *C. sp. D*. Thus, although the x2cb sequences of *C. sp. C* and *C. sp. D* are essential to confirm our observations, we strongly encourage the use of the x2cb fragment as a new molecular marker in future analyses on *Ciona* species.

In conclusion, our results indicate an integrative taxonomic approach, involving the analysis of morphological, ecological and molecular characters, as a fundamental requirement for the delineation and description of new *Ciona* species. This is in accordance with previous studies of *Ciona*, where molecular data were crucial for addressing morphological re-analyses and taxonomic revisions (Suzuki *et al.*, 2005; Caputi *et al.*, 2007; Iannelli *et al.*, 2007; Nydam & Harrison, 2007, 2010; Zhan *et al.*, 2010; Sato *et al.*, 2012; Brunetti *et al.*, 2015; Pennati *et al.*, 2015; Gissi *et al.*, 2017; Malfant *et al.*, 2018). In view of these results, the ‘*Ciona* case’ is still far from being resolved, but the present study brings us a step forwards.

#### ACKNOWLEDGEMENTS

This work was partially supported by the Ministero dell’Istruzione, dell’Università e della Ricerca (MIUR), Italy, to Ca.Gi., who also acknowledges the support of the Molecular Biodiversity Laboratory of the Italian node of Lifewatch (Consiglio Nazionale delle Ricerche CNR). Gi. Ch. is supported by MIUR, Italy, project of the Programma Operativo Nazionale (PON) 2014-2020 (AIM1807508-1, Linea 1). F.V. acknowledges support from the Agence Nationale de la Recherche (ANR), project “Hybridisation in the Sea” (HySea) (No. ANR-12-BSV7-0011). The authors thank Marie Nydam for helpful discussion and photographic material; and Maarten Christenhusz, Monika Böhm, Xavier Turon and an anonymous reviewer for their useful suggestions. The authors declare that they have no conflict of interest.

#### REFERENCES

- Ahrens D, Fujisawa T, Krammer HJ, Eberle J, Fabrizi S, Vogler AP. 2016. Rarity and incomplete sampling in DNA-based species delimitation. *Systematic Biology* **65**: 478–494.
- Altschul SF, Gish W, Miller W, Myers EW, Lipman DJ. 1990. Basic local alignment search tool. *Journal of Molecular Biology* **215**: 403–410.
- Berrill NJ. 1950. *The Tunicata with an account of the British species*. London: Ray Society publications.
- Bouchemousse S, Bishop JD, Viard F. 2016a. Contrasting global genetic patterns in two biologically similar, widespread and invasive *Ciona* species (Tunicata, Ascidiacea). *Scientific Reports* **6**: 24875.
- Bouchemousse S, Lévêque L, Dubois G, Viard F. 2016b. Co-occurrence and reproductive synchrony do not ensure hybridization between an alien tunicate and its interfertile native congener. *Evolutionary Ecology* **30**: 69–87.
- Bouchemousse S, Liautard-Haag C, Bierne N, Viard F. 2016c. Distinguishing contemporary hybridization from past introgression with postgenomic ancestry-informative SNPs in strongly differentiated *Ciona* species. *Molecular Ecology* **25**: 5527–5542.
- Brunetti R, Gissi C, Pennati R, Caicci F, Gasparini F, Manni L. 2015. Morphological evidence that the molecularly determined *Ciona intestinalis* type A and type B are different species: *Ciona robusta* and *Ciona intestinalis*. *Journal of Zoological Systematics and Evolutionary Research* **53**: 186–193.
- Brunetti R, Manni L, Mastrototaro F, Gissi C, Gasparini F. 2017. Fixation, description and DNA barcode of a neotype for *Botryllus schlosseri* (Pallas, 1766) (Tunicata, Ascidiacea). *Zootaxa* **4353**: 29–50.
- Brunetti R, Mastrototaro F. 2017. *Ascidiacea of the European waters*. Milan: Edagricole – New Business Media II.
- Cañestro C, Bassham S, Postlethwait JH. 2003. Seeing chordate evolution through the *Ciona* genome sequence. *Genome Biology* **4**: 208.
- Caputi L, Andreakis N, Mastrototaro F, Cirino P, Vassillo M, Sordino P. 2007. Cryptic speciation in a model invertebrate chordate. *Proceedings of the National Academy of Sciences of the United States of America* **104**: 9364–9369.
- Copello M, Devos L, Lafargue F. 1981. *Ciona edwardsi* (Roule, 1886) espèce littorale de Méditerranée et distincte de *Ciona intestinalis* Linné, 1767. *Vie Milieu* **31**: 243–253.
- Dehal P, Satou Y, Campbell RK, Chapman J, Degnan B, De Tomaso A, Davidson B, Di Gregorio A, Gelpke M, Goodstein DM, Harafuji N. 2002. The draft genome of *Ciona intestinalis*: insights into chordate and vertebrate origins. *Science* **298**: 2157–2167.
- Dybern BI. 1967. The distribution and salinity tolerance of *Ciona intestinalis* (L.) f. *typica* with special reference to the waters around southern Scandinavia. *Ophelia* **4**: 207–226.
- Gissi C, Hastings KE, Gasparini F, Stach T, Pennati R, Manni L. 2017. An unprecedented taxonomic revision of a model organism: the paradigmatic case of *Ciona robusta* and *Ciona intestinalis*. *Zoologica Scripta* **46**: 521–522.
- Gissi C, Pesole G, Mastrototaro F, Iannelli F, Guida V, Griggio F. 2010. Hypervariability of ascidian mitochondrial gene order: exposing the myth of deuterostome organelle genome stability. *Molecular Biology and Evolution* **27**: 211–215.
- Guindon S, Gascuel O. 2003. A simple, fast, and accurate algorithm to estimate large phylogenies by maximum likelihood. *Systematic Biology* **52**: 696–704.
- Hancock A. 1870. On the larval state of *Molgula*; with descriptions of several new species of simple ascidians. *Annals of Natural History, fourth series* **6**: 353–368.
- Harant H, Vernières P. 1933. *Faune de France 27. Tuniciers fascicule 1: Ascidies*. Paris: Paul Lechevalier.

- Hartmeyer R. 1909–1911.** Ascidiens. In: Bronn HG. *Klassen und Ordnungen des Tier-Reichs*, Vol. 3. Leipzig: C.F. Winter'sche Verlagshandlung.
- Hartmeyer R. 1911.** Die Ascidiens der Deutschen Südpolar Expedition 1901–1903. *Deutsche Sudpolar-Expedition* 12: 403–606.
- Hawkins CJ, Kott P, Parry DL, Swinehart JH. 1983.** Vanadium content and oxidation state related to ascidian phylogeny. *Comparative Biochemistry and Physiology Part B: Comparative Biochemistry* 76: 555–558.
- Hebert PD, Cywinska A, Ball SL, deWaard JR. 2003.** Biological identifications through DNA barcodes. *Proceedings of the Royal Society B: Biological Sciences* 270: 313–321.
- Hebert PD, Stoeckle MY, Zemplak TS, Francis CM. 2004.** Identification of birds through DNA barcodes. *PLoS Biology* 2: e312.
- Herdman WA. 1882.** Report on the Tunicata collected during the voyage of HMS Challenger during the years 1873–76. I. Ascidiæ simplices. *Report of the Scientific Results of the Voyage of HMS Challenger during the Years 1873–76* 6: 1–296.
- Hirose M, Hirose E. 2009.** DNA barcoding in photosymbiotic species of *Diplosoma* (Ascidiacea: Didemnidae), with the description of a new species from the southern Ryukyus, Japan. *Zoological Science* 26: 564–568.
- Hoshino ZI, Nishikawa T. 1985.** Taxonomic studies of *Ciona intestinalis* (L.) and its allies. *Publication of the Seto Marine Biological Laboratory* 30: 61–79.
- Hoshino ZI, Tokioka T. 1967.** An unusually robust *Ciona* from the northeastern coast of Honsyu Island, Japan. *Publication of the Seto Marine Biological Laboratory* 15: 275–290.
- Iannelli F, Pesole G, Sordino P, Gissi C. 2007.** Mitogenomics reveals two cryptic species in *Ciona intestinalis*. *Trends in Genetics* 23: 419–422.
- ICZN. 1999.** *International code of zoological nomenclature, 4th Edition*. London: The International Trust for Zoological Nomenclature, The Natural History Museum.
- Jukes TH, Cantor CR. 1969.** Evolution of protein molecules. *Mammalian Protein Metabolism* 3: 22–126.
- Katoh K, Misawa K, Kuma K, Miyata T. 2002.** MAFFT: a novel method for rapid multiple sequence alignment based on fast Fourier transform. *Nucleic Acids Research* 30: 3059–3066.
- Kearse M, Moir R, Wilson A, Stones-Havas S, Cheung M, Sturrock S, Buxton S, Cooper A, Markowitz S, Duran C, Thierer T, Ashton B, Meintjes P, Drummond A. 2012.** Geneious Basic: an integrated and extendable desktop software platform for the organization and analysis of sequence data. *Bioinformatics* 28: 1647–1649.
- Kekkonen M, Hebert PD. 2014.** DNA barcode-based delineation of putative species: efficient start for taxonomic workflows. *Molecular Ecology Resources* 14: 706–715.
- Kekkonen M, Mutanen M, Kaila L, Nieminen M, Hebert PDN. 2015.** Delineating species with DNA barcodes: a case of taxon dependent method performance in moths. *PLoS One* 10: e0122481.
- Kimura M. 1980.** A simple method for estimating evolutionary rates of base substitutions through comparative studies of nucleotide sequences. *Journal of Molecular Evolution* 16: 111–120.
- Kott P. 1990.** *The Australian Ascidiacea. Part 2, Aplousobranchia (1)*. Brisbane: Memoirs of the Queensland Museum.
- Kott P. 2005.** *Catalogue of Tunicata in Australian waters*. Canberra: Australian Biological Resources Study.
- Lahille F. 1890.** *Recherches sur les tunicier des côtes de France*. Toulouse: Imprimerie Lagarde et Sebille.
- Lambert C, Lafargue F, Lambert G. 1990.** Preliminary note on the genetic isolation of *Ciona* species (Ascidiacea, Urochordata). *Vie Milieu* 40: 293–295.
- Lefort V, Longueville JE, Gascuel O. 2017.** SMS: smart model selection in PhyML. *Molecular Biology and Evolution* 34: 2422–2424.
- Lemaire P. 2011.** Evolutionary crossroads in developmental biology: the tunicates. *Development* 138: 2143–2152.
- Lim GS, Balke M, Meier R. 2012.** Determining species boundaries in a world full of rarity: singletons, species delimitation methods. *Systematic Biology* 61: 165–169.
- Malfant M, Darras S, Viard F. 2018.** Coupling molecular data and experimental crosses sheds light about species delineation: a case study with the genus *Ciona*. *Scientific Reports* 8: 1480.
- Mastrototaro F, D'Onghia G, Tursi A. 2008.** Spatial and seasonal distribution of ascidians in a semi-enclosed basin of the Mediterranean Sea. *Journal of the Marine Biological Association of the United Kingdom* 88: 1053–1061.
- Mastrototaro F, Montesanto F, Salonna M, Grieco F, Trainito E, Chimienti G, Gissi C. 2019.** Hitch-hikers of the sea: concurrent morphological and molecular identification of *Symplegma brakenhielmi* (Tunicata: Ascidiacea) in the western Mediterranean Sea. *Mediterranean Marine Science* 20: 197–207.
- Mastrototaro F, Relini G. 2011.** Prima segnalazione di *Ciona edwardsi* (Roule, 1886) (Tunicata, Ascidiacea) in Mar Ligure. First record of *Ciona edwardsi* (Roule, 1886) (Tunicata, Ascidiacea) in the Ligurian Sea. *Biologia Marina Mediterranea* 18: 262.
- Mastrototaro F, Tursi A, Costantino G. 2000.** Ascidiacei della riserva marina di Ustica. *Biologia Marina Mediterranea* 7: 691–694.
- Millar RH. 1953.** *Ciona. LMBC memoirs on typical British marine plants and animals, Vol. 35*. Liverpool: Liverpool University Press.
- Monniot C. 1963.** Presence a Bergen de *Ciona fascicularis* Hancock, 1870. *Sarsia* 11: 5–9.
- Monniot C. 1991.** Ascidiens de Nouvelle-Calédonie. 8. Phlebobraches (suite). *Bulletin du Muséum National d'Histoire Naturelle* 4: 491–515.
- Monniot C. 1998.** Abyssal ascidians collected from the proximity of hydrothermal vents in the Pacific Ocean. *Bulletin of Marine Science* 63: 541–558.
- Monniot C, Monniot F. 1983.** Ascidiens antarctiques et subantarctiques: morphologie et biogéographie. *Mémoires du Muséum National d'Histoire Naturelle* 125: 1–168.
- Monniot C, Monniot F. 1989.** Ascidiens collected around the Galapagos Islands using the Johnson-Sea-Link research

- submersible. *Proceedings of the Biological Society of Washington* **102**: 14–32.
- Monniot F, Dettai A, Eleaume M, Cruaud C, Ameziane N. 2011.** Antarctic Ascidians (Tunicata) of the French-Australian survey CEAMARC in Terre Adélie. *Zootaxa* **2817**: 1–54.
- Monniot F, Monniot C. 2001.** Ascidians from the tropical western Pacific. *Zoosystema* **23**: 201–383.
- Nydam ML, Harrison RG. 2007.** Genealogical relationships within and among shallow-water *Ciona* species (Ascidiacea). *Marine Biology* **151**: 1839–1847.
- Nydam ML, Harrison RG. 2010.** Polymorphism and divergence within the ascidian genus *Ciona*. *Molecular Phylogenetics and Evolution* **56**: 718–726.
- Ordóñez V, Pascual M, Fernández-Tejedor M, Turon X. 2016.** When invasion biology meets taxonomy: *Clavelina oblonga* (Ascidiacea) is an old invader in the Mediterranean Sea. *Biological Invasions* **18**: 1203–1215.
- Padial JM, Miralles A, De la Riva I, Vences M. 2010.** The integrative future of taxonomy. *Frontiers in Zoology* **7**: 16.
- Pennati R, Ficetola GF, Brunetti R, Caicci F, Gasparini F, Griggio F, Sato A, Stach T, Kaul S, Gissi C, Manni L. 2015.** Morphological differences between larvae of the *Ciona intestinalis* species complex: hints for a valid taxonomic definition of distinct species. *PLoS One* **10**: e0122879.
- Procaccini G, Affinito O, Toscano F, Sordino P. 2011.** A new animal model for merging ecology and evolution. In: Pontarotti P, ed. *Evolutionary biology – concepts, biodiversity, macroevolution and genome evolution*. Berlin, Heidelberg: Springer, 91–106.
- Puillandre N, Lambert A, Brouillet S, Achaz G. 2012.** ABGD, Automatic Barcode Gap Discovery for primary species delimitation. *Molecular Ecology* **21**: 1864–1877.
- Ramos-Esplá AA, Cárcel JA, Varela M. 2005.** Zoogeographical relationships of the littoral ascidiofauna at the Antarctic peninsula, in the Scotia Arc and in the Magellan region. *Scientia Marina* **69**: 215–223.
- Ronquist F, Teslenko M, van der Mark P, Ayres DL, Darling A, Höhna S, Huelsenbeck JP. 2012.** MrBayes 3.2: efficient Bayesian phylogenetic inference and model choice across a large model space. *Systematic Biology* **61**: 539–542.
- Roux C, Tsigkogeorga G, Bierne N, Galtier N. 2013.** Crossing the species barrier: genomic hotspots of introgression between two highly divergent *Ciona intestinalis* species. *Molecular Biology and Evolution* **30**: 1574–1587.
- Rubinstein ND, Feldstein T, Shenkar N, Botero-Castro F, Griggio F, Mastrototaro F, Delsuc F, Douzery EJ, Gissi C, Huchon D. 2013.** Deep sequencing of mixed total DNA without barcodes allows efficient assembly of highly plastic ascidian mitochondrial genomes. *Genome Biology and Evolution* **5**: 1185–1199.
- Sanamyan K. 1998.** Ascidians from the north-western Pacific region. 5. Phlebobranchia. *Ophelia* **49**: 97–116.
- Sanamyan K, Sanamyan N. 2007.** Poorly known Ascidiacea collected in the vicinity of the Commander Islands and east Kamchatka, NW Pacific. *Zootaxa* **1579**: 55–68.
- Sato A, Satoh N, Bishop JDD. 2012.** Field identification of ‘types’ A and B of the ascidian *Ciona intestinalis* in a region of sympatry. *Marine Biology* **159**: 1611–1619.
- Sato A, Shimeld SM, Bishop JD. 2014.** Symmetrical reproductive compatibility of two species in the *Ciona intestinalis* (Ascidiacea) species complex, a model for marine genomics and developmental biology. *Zoological Science* **31**: 369–374.
- Satoh N, Satou Y, Davidson B, Levine M. 2003.** *Ciona intestinalis*: an emerging model for whole-genome analyses. *Trends in Genetics* **19**: 376–381.
- Shenkar N, Koplovitz G, Dray L, Gissi C, Huchon D. 2016.** Back to solitude: solving the phylogenetic position of the Diazonidae using molecular and developmental characters. *Molecular Phylogenetics and Evolution* **100**: 51–56.
- Smith MA, Fisher BL, Hebert PD. 2005.** DNA barcoding for effective biodiversity assessment of a hyperdiverse arthropod group: the ants of Madagascar. *Philosophical Transactions of the Royal Society B: Biological Sciences* **360**: 1825–1834.
- Suzuki MM, Nishikawa T, Bird A. 2005.** Genomic approaches reveal unexpected genetic divergence within *Ciona intestinalis*. *Journal of Molecular Evolution* **61**: 627–635.
- Talavera G, Dincă V, Vila R. 2013.** Factors affecting species delimitations with the GMYC model: insights from a butterfly survey. *Methods in Ecology and Evolution* **4**: 1101–1110.
- Tang CQ, Humphreys AM, Fontaneto D, Barraclough TG. 2014.** Effects of phylogenetic reconstruction method on the robustness of species delimitation using single-locus data. *Methods in Ecology and Evolution* **5**: 1086–1094.
- Tsigkogeorga G, Turon X, Galtier N, Douzery EJ, Delsuc F. 2010.** Accelerated evolutionary rate of housekeeping genes in tunicates. *Journal of Molecular Evolution* **71**: 153–167.
- Turon X, López-Legentil S. 2004.** Ascidian molecular phylogeny inferred from mtDNA data with emphasis on the Aplousobranchiata. *Molecular Phylogenetics and Evolution* **33**: 309–320.
- Van Name WG. 1945.** The North and South American ascidians. *Bulletin of the American Museum of Natural History* **84**: 1–476.
- Yokobori Si, Ueda T, Feldmaier-Fuchs G, Pääbo S, Ueshima R, Kondow A, Nishikawa K, Watanabe K. 1999.** Complete DNA sequence of the mitochondrial genome of the ascidian *Halocynthia roretzi* (Chordata, Urochordata). *Genetics* **153**: 1851–1862.
- Zhan A, Briski E, Bock D, Ghabooli S, MacIsaac H. 2015.** Ascidiaceans as models for studying invasion success. *Marine Biology* **162**: 2449–2470.
- Zhan A, Macisaac HJ, Cristescu ME. 2010.** Invasion genetics of the *Ciona intestinalis* species complex: from regional endemism to global homogeneity. *Molecular Ecology* **19**: 4678–4694.
- Zhang J, Kapli P, Pavlidis P, Stamatakis A. 2013.** A general species delimitation method with applications to phylogenetic placements. *Bioinformatics* **29**: 2869–2876.

## SUPPORTING INFORMATION

Additional Supporting Information may be found in the online version of this article at the publisher's web-site:

**Table S1.** Specimens of *Ciona edwardsi*, *Ciona intestinalis* and *Ciona robusta* from the private collection of F. Mastrototaro examined in this study. Number of samples, collection site and identifiers are also reported.

**Table S2.** List of the aligned *cox1* sequences. Red colour indicates sequences produced in the present study. Sequences excluded and included in the alignment '737-Nogap-47taxa' and '1084-12taxa', respectively, are also reported.

**Table S3.** List of the *cox2* and *cob* sequences included in the alignment of the x2cb fragment. Red colour indicates sequences produced in the present study. Abbreviation: ORF, open reading frame.

**Table S4.** List of the sequences included in the alignment of the x3n1 fragment. Red colour indicates sequences produced in the present study.

**Table S5.** Results of the automatic barcode gap discovery (ABGD) analyses on the four *cox1* alignments and on the x3n1 alignment using the default values for parameters  $X$  and  $P_{min}$ – $P_{max}$ . The few differences for results obtained with  $X = 1, 2$  or  $3$  are also reported within brackets. The 'no. of expected OTUs' includes one OTU for *Ciona intermedia* and one OTU for the clade joining *Ciona intestinalis* with *Ciona roulei*. Red indicates values different from those expected; curved brackets indicate content of unexpected OTUs merging several species; square brackets indicate different results obtained with  $X = 1$ ; curly brackets indicate different results obtained with  $X = 2$  and  $X = 3$ . Abbreviations: Init, initial partitions; nd, not determined; OTU, operational taxonomic unit; Rec, recursive partitions.